HIGH RESOLUTION STRATIGRAPHY AND FACIES ARCHITECTURE OF BUDA FORMATION IN CENTRAL TEXAS

A Thesis

by

XIAODONG ZHANG

Submitted to the Office of Graduate and Professional Studies of
Texas A&M University
in partial fulfillment of the requirements for the degree of

MASTER OF SCIENCE

Chair of Committee,	Michael Pope
Committee Members,	Juan Carlos Laya
	Zoya Heidari
Head of Department,	Michael Pope

August 2017

Major Subject: Geology

ABSTRACT

The Upper Cretaceous Buda Formation in central Texas is overlain by Eagle Ford group (or False Buda unit locally), and overlying the Del Rio Formation (Grayson Formation). The Buda Formation outcrop exposes from west Texas to the Dallas-Forth Worth area, and extends continuously into subsurface in central Texas. This study focuses on subsurface stratigraphy of the Buda Formation based on core analysis and outcrop descriptions to determine the regional distribution of depositional environment of the Buda Formation in central Texas.

Three facies (from deep to shallow) are interpreted from core to outcrops: foraminfera mudstone, skeletal wackestone/packstone, and massive mudstone. Outcrops are mainly composed of skeletal wackestone with massive mudstone, whilst cores are dominated by *globigerinid* mudstone and skeletal wackestone/packstone. Both outcrops and cores are extremely burrow mottled. The abundance of bioturbation and benthic forams across the depositional profile suggests deposition occurred along a well-oxygenated, low relief ramp.

2D strike and dip cross sections constrained by cores indicate that the thickness of the Buda Formation varies significantly from 20 to 100 feet through central Texas. Considerable thickening of the Buda Formation within the trough between Edwards and Sligo paleo shelf margins occurs in south Wilson, north Karnes and Gonzales counties of central Texas. The dramatic variations of the Buda Formation thickness along the dip direction are consistent with filling differential accommodation space across the paleotopographic profile of the pre-existing Lower Cretaceous reef trend. Depositional

pattern shown on cross-section indicates possible transgression sequence followed by Eagle Ford transgression.

Typical reversed "J" pattern shows the relationship of $\delta^{13}C_{vPDB}$ and $\delta^{18}O_{vPDB}$ from core samples indicating the Buda Formation definitely being altered under meteoric conditions during diagenetic process. Cathodoluminescence results indicate two diagenetic events occurred in Buda Formation from early marine cementation to burial diagenesis under marine-meteoric mixing water conditions based on two luminesces color stages from dull to bright orange.

The False Buda unit (locally overlying the Buda Formation in central Texas) is quite similar to Maness shale (equally to lower Eagle Ford group in south Texas) composed of low Ca but high Si, Al, K based on geochemical analysis. Large negative excursion event is shown around the Lower Eagle Ford-False Buda contact, which possibly indicates that subaerial exposure or marine erosion occurred during sedimentation.

DEDICATION

This thesis is dedicated to my family in China, and my fiancé Zhen Yin in Edinburgh, UK.

ACKNOWLEDGEMENTS

I would like to thank my committee chair, Dr. Michael Pope, and my committee members, Dr. Laya, and Dr. Heidari, for their guidance and support throughout the course of this research.

Thanks also go to my friends and colleagues and the department faculty and staff for making my time at Texas A&M University a great experience.

Special thanks to SM Energy for providing me with core data and helping this project accomplish.

Finally, thanks to my family for their encouragement and to my fiancé for his patience and love.

CONTRIBUTORS AND FUNDING SOURCES

This work was supported by a thesis committee consisting of Professor Michael Pope and Dr. Laya of the Department of Geology & Geophysics and Professor Dr. Heidari of the Department of Petroleum Engineering.

Graduate study was supported by a graduate assistantship from Department of Geology & Geophysics at Texas A&M University.

All work conducted for the thesis that was completed by the student independently.

TABLE OF CONTENTS

Page

LIST OF FIGURES

Page

CHAPTER I

INTRODUCTION

The Buda Formation has a long production history since the 1930s in central Texas (Dickey, 1983). A review from Texas Railroad Commission production report indicates that around 2 billion barrels of oil were produced from Buda Formation in Satin-Lott, Chilton oil fields of Falls County in central Texas since 1930s. However, the Giddings field in Lee County (Horstmann, 1987) also was evaluated Buda Formation as a large potential play back in 1980s but only few completed wells produced more than 25,000 barrels per year. Variable production performance of Buda reservoir by counties may be due to fracture and fault controlled reservoir properties that are caused by local structural displacement. Although production from the Buda Formation is widespread in central Texas, its desirable production occurs only where the porous and fractured limestone are both in favorable combination. The productive interval of Buda Formation is mainly concentrated in discontinuous band/traps of minor reservoirs extending in southwestern direction in central Texas (Turner, 1950). This complicated stratigraphic trap pattern, limited by fracture and fault reservoir type, is very difficult for conventional drilling exploitation. Extensive local diagenesis and secondary porosity development make the Buda Formation reservoir even more complicated to characterize its reservoir properties regionally. Increased use of low cost hydraulic fracturing and horizontal drilling in recent years enable industry to more efficiently exploit the Buda Formation reservoir with natural fracture systems compared to Eagle Ford or Austin chalk.

This study focuses on core analysis, wireline log analysis and outcrop descriptions to determine the sequence stratigraphic framework of the Buda Formation. Integrating abundant subsurface data (core and wireline logs) with the outcrop studies provides understanding of the regional depositional architecture. 3D depositional model calibrated with cores and wireline logs of the Buda Formation additionally provides a more complete understanding of its surface to subsurface depositional environment. Diagenetic study of the Buda Formation in central Texas aims to study local porosity and permeability variations of cores to better understand regional reservoir features. It is critical to determine diagenetic events with petrographic and geochemical methods (e.g. stable isotope, XRF, CL etc.) for temporally understand its burial history.

CHAPTER II

GEOLOGICAL BACKGROUND

During Late Cenomanian to Early Turonian (90 to 100 Ma), warm climate and development of anoxic ocean conditions (Figure 1) resulted in large accumulations of organic carbon (Montgomery, 1990). The syndepositional San Marcos Arch separates the Maverick Basin in south-central Texas and the East Texas Basin during the Late Cretaceous when a large carbonate platform developed (Luttrell, 1977). During most of the Cretaceous, the San Marcos Arch was a low-lying subaerial terrain with little sediment supply (Young, 1986). The study area of Buda Formation is located west of the San Marcos Arch in subsurface and outcrops in west and central Texas (Figure 2). Multiple syntectonic uplifts and depressions influenced depositional environments of the Buda Formation, and likely contributed to its variable thickness distribution across Texas (ranging from < 1 m to > 50 m). The Balcones faults system trending along the Paleozoic Quachita fold and thrust belt coincides with the Buda Formation outcrop belt in central Texas near San Antonio area. Parallel to the Balcones fault systems further southeastward is the Luling-Mexia-Talco fault systems that produced horst and graben structures with conjugate normal faults dipping to the southeast and northwest direction (Culotta et al., 1992). The subsurface deposition of the Buda Formation in this study area was affected by the local Luling-Mexia-Talco fault systems.

The Buda Formation unconformably overlies the Georgetown Limestone or locally the Del Rio Formation in west Texas. The pre-existing Sligo and Edwards carbonate platforms had a high relief rudist rimmed shelf margins underlying the Del

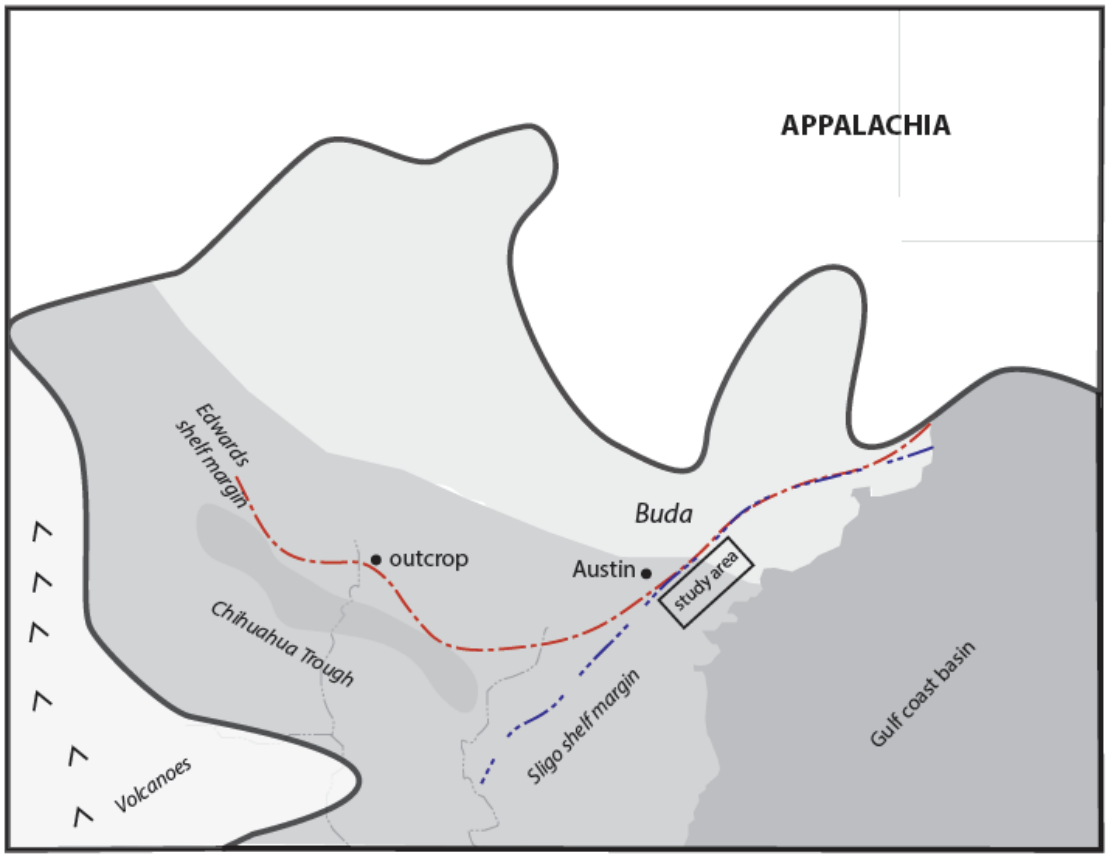

Figure 1. Paleogeographic map of Late Cenomanian (96~100 ma) is shown where Buda Formation deposited. Two paleo shelf margin Sligo and Edward outlined during the Buda deposition.

Rio Formation (Ryan M Phelps et al., 2014)In central Texas, the subsurface cores show the Buda Formation conformably overlying the Del Rio Formation. Throughout Texas, the Del Rio Formation was deposited in a near-shore, low energy shallow marine to brackish-water environment with clastic influx from northeast Texas (Hover, Bases, & and Lock, 2008). The influx especially altered the Del Rio/Grayson Formation sedimentation in southwest Texas, which brought to the end of Sligo and Edwards carbonate platform (Hover et al., 2008). Marine transgression was initiated, probably

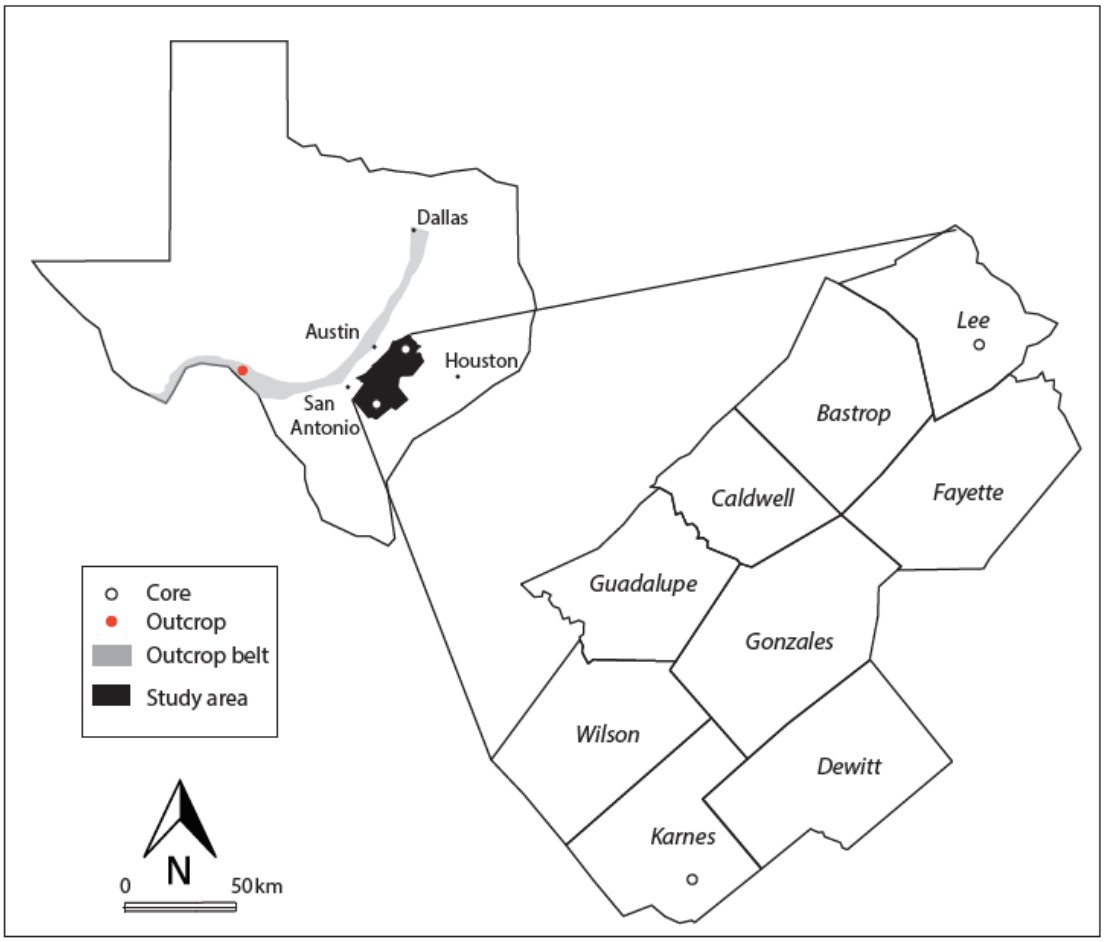

Figure 2. Study area of Buda Formation in central Texas. Gray color shows the outcrop belt of Buda Formation across Texas. Two cores are located in Lee and Karnes counties respectively. One outcrop was measured in west Texas near Del Rio.

from south structural features, resulted in reduction of extent of open ocean circulation during Grayson Formation in north central Texas. Southwest Texas was least affected by marine invasion to keep neritic conditions persisted. The periodic deposition of carbonate lime mud marked a return to optimum open marine conditions during the Buda Formation deposition (Mancini, 1977). The Lower Eagle Ford group unconformably overlies the Buda Formation (Figure 3) with the regional Mid-

Cenomanian unconformity contact (Reaser & Dawson, 1995). A major transgression of the Comanchean shelf in the middle to late Cenomanian initiated the deposition of the Eagle Ford Group after the regression depositional cycle of the Buda Formation (R. M Phelps, 2011; Sohl, 1991)

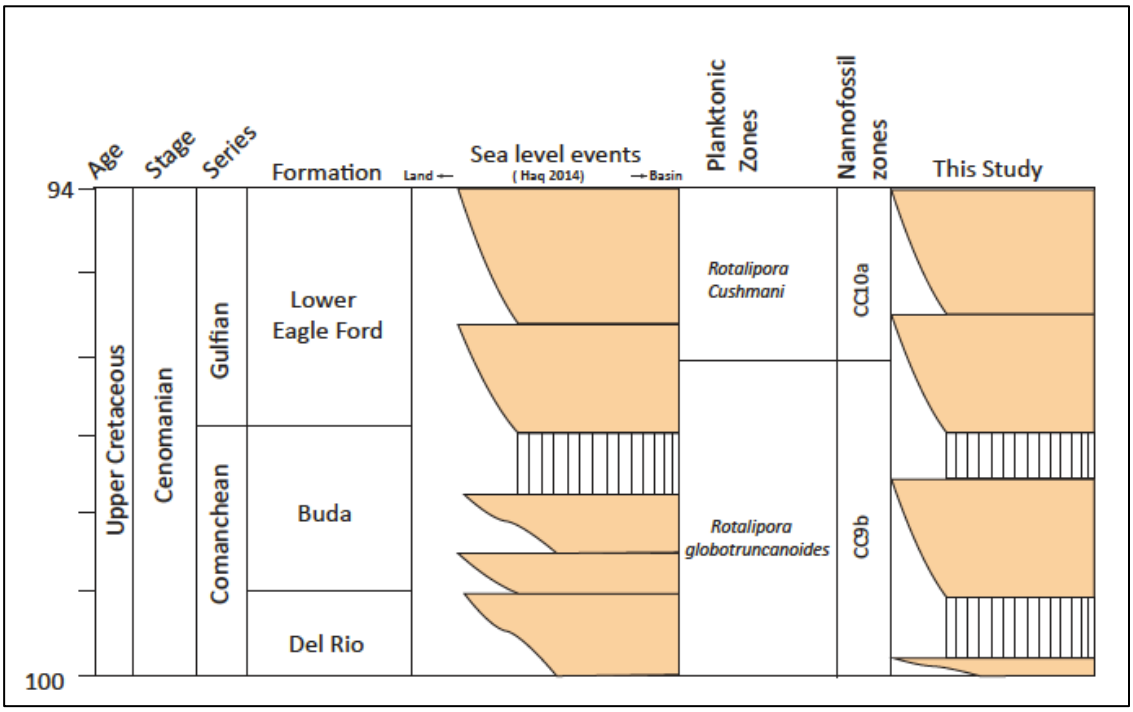

Figure 3. Stratigraphic column of Comanchean and Gulfian series of Upper Cretaceous in central Texas. The Buda Formation is in Late Comanchean Series around 98 to 100 ma. (Adapted from Haq (2014)

Previous research (Brown, 1971; Erdogan, 1969; Martin, 1961; Young, 1967; Zink, 1957), indicates the Buda Formation has a substantial uniform lithology sub-divided into two distinct depositional facies based on different fossil assemblages: calcareous foraminifera wackestone and globigerinid algal mudstone. Complete drowning of the reef margin occurred during deposition of early Cenomanian flooded

shale facies Del Rio Formation and carbonates Buda Formation (Phelps et al. 2014). Due to conformable relation of Del Rio and Buda Formation in subsurface central Texas, Previous work (Scott, Benson, Morin, Shaffer, & and Oboh-Ikuenobe, 2003) (E. A. Mancini, Obid, Badali, Liu, & and Parcell, 2008) proposed that the highstand system cycle of Edwards group and flooded facies of Del Rio and Buda are tentatively grouped into one single stratigraphic Transgressive-Regressive cycle. The depositional environmental conditions during the Buda deposited was more stable than that of Del Rio and represents a return to a more open marine environment, interpreted as a gradual transgression of a shallow warm Cretaceous sea (Lock, Grimball, & Johnson, 2013)

In the study area, a dark argillaceous limestone unit informally known as the False Buda was deposited conformably above the Buda Formation. Previous research indicate this unit is correlative with the Maness Shale Formation that generally was included into the Lower Eagle Ford in south Texas (Hentz & Ruppel, 2010).

CHAPTER III

METHODS

Field method

Several outcrop exposures of Buda Formation in west and central Texas were measured bed-by-bed to describe rock textures and bedding structures for surface stratigraphy in order to further correlate with subsurface cores in central Texas. Outcrop samples were collected systematically every 6 inches (15 cm) for geochemical analysis. A handheld Gamma Ray scintillometer was used to determine the radiometric concentrations of K, Th and U elements on the bedding. Detailed outcrop descriptions and gamma ray profiles characterize the surface sequence stratigraphic framework to help better understand depositional environments and correlations with subsurface Buda Formation. Two cores from central Texas were analyzed with detailed facies description and geochemical methods to make regional correlation with outcrops in west Texas.

Petrographic Analysis

Samples from cores in Lee and Karnes counties were sent to Applied Petrographic Lab in Pennsylvania for thin section preparation. Each sample was selected to represent specific rock type, depositional facies and sedimentary structures such as channel fills and bioturbation. The thin sections were analyzed with a Nikon Eclipse E400 petrographic microscope under plain polarized transmitted light. High-resolution illustration of matrix and skeletal grains is critical to identify rock facies and microfossil types. Based on similar facies and microscopic features of cores and outcrops, regional

correlation (from surface to subsurface) can be performed to determine the distribution of depositional environments in central Texas.

Stable Isotope

Diagenetic environments of the carbonate rocks can be recorded isotopically by cement generations of distinct isotopic composition (Hudson 1977). 33 whole rock samples were collected from core and outcrops of Buda Formation for $\delta^{13}C_{vPDB}$ and $\delta^{18}O_{vPDB}$ analysis. In addition, 8 samples from the Del Rio-Buda Formations and Buda-Eagle Ford Formations contacts were collected to determine if the contacts were subaerially exposed. The stable isotope analysis was performed with a high-precision Thermo Finnigan Kiel IV carbonate device coupled to a Thermo Finnigan MAT 253 dual inlet isotope ratio mass spectrometer. The analytical uncertainties are 0.04 ‰ of $\delta^{13}C_{vPDB}$ and 0.06% of $\delta^{18}O_{vPDB}$ for normal sized samples based on long term daily measurements of the international carbonate standard NBS-19. The Kiel IV devices use the principle of individual acid baths, storage, transfer and chemical reaction of phosphoric acid at elevated temperature controls.

Cathodoluminescence (CL)

The cathodoluminescent zones in the cements of carbonate rocks commonly are formed in ancient limestone successions (Pagel et al. 2000). The luminescence of minerals that compose the cements are interpreted as responses of variable redox conditions of formative pore waters during crystal growth. Cathodoluminescence (CL) analysis uses electrons impacting minerals cements to examine the distributions of luminescent features (Pagel et al. 2000). Based on different luminescent features,

concentration of major activator Fe^{2+} and receiver Mn^{2+} elements can be estimated with colors (Boggs & Krinsley, 2006). Different color zones represents different cementation and burial conditions, for example, for the redox-reduced conditions the color range will be blackish, while for the oxidized conditions the color could be bright to dull to reddish (Gotze 2002). Combined with the physical patterns of cements, CL analysis is an additional petrographic tool to better understand the diagenetic events (e.g. dissolution, cementation, or compaction).

Correlation

The surface to subsurface correlation of the Buda Formation is the key procedure to construct its 3D depositional model with high-resolution facies analysis of outcrop and core. Wireline log correlations are calibrated with cores in subsurface through facies. An isochore map was generated with Gamma Ray (GR) and resistivity logs to show the thickness distribution of the Buda Formation in study area. Parasequences were identified according to rock facies in the core, and wireline log patterns. The parasequences were integrated into the depositional architecture to determine the sequence stratigraphy framework with core and wireline log restricted in central Texas. Flooding surfaces recorded by shale layers both observed in the outcrop and cores is helpful to redefine the depositional model together with detailed sequence stratigraphy analysis.

CHAPTER IV

DATA

Outcrop data

One outcrop section was measured along highway 90 near Seminole Canyon State Park, Val Verde County, west Texas. Two outcrops were revisited near San Antonio and Austin area (Ak, 2015), (Fairbanks, Ruppel, & Rowe, 2016) to better understand the local surface stratigraphy and compare with subsurface core data in central Texas (Figure 4). A spectral GR log profile was constructed using a hand-held scintillometer with a sampling interval of 1 ft (30 cm) vertically along the outcrop bedding in order to better correlate the Buda Formation with borehole gamma ray log data.

Subsurface data

Two cores (one in Lee and one in Karnes County) were described bed-by-bed for rock textures, bedding structures, bioturbation intensity at millimeter scales in central Texas. For regionally correlation purpose, two outcrops in San Antonio and Austin from previous work also are used to correlate with cores to have a complete facies map (Figure 5). Wireline log data were acquired from the Drillinginfo database by counties. Gamma Ray (GR), and resistivity logs are major log types used in the wireline log correlations. Low GR values coincident with high Resistivity values throughout the middle Buda Formation is a typical pattern shown in the wireline log (Figure 6). To obtain a regional perspective of the depositional architecture, two dip cross sections were

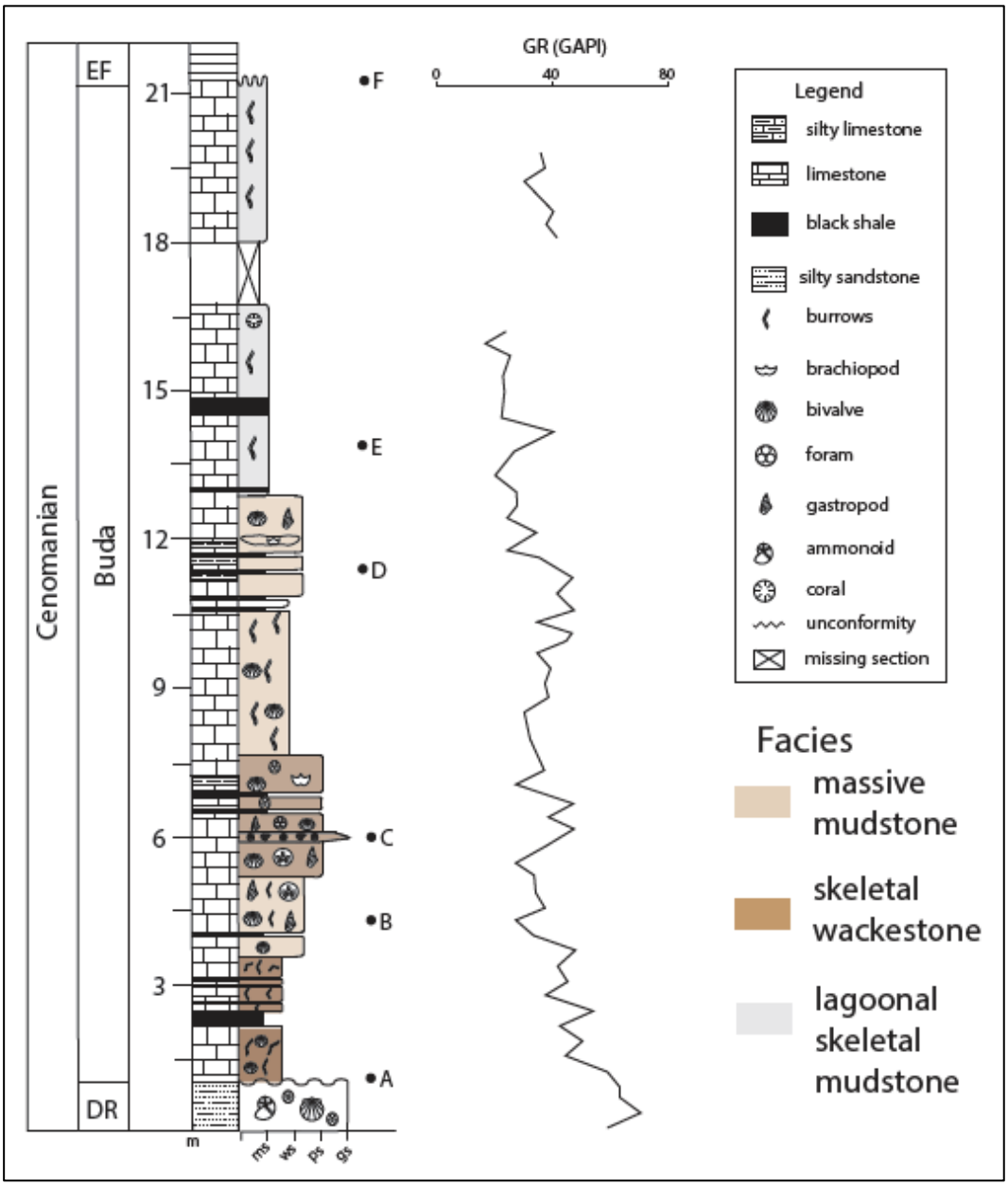

Figure 4. Outcrop measurement of Buda Formation in west Texas with hand-held GR data. Two facies identified from outcrop samples: Massive mudstone and skeletal wackestone. Major fossil groups include bivalve, gastropod, foraminifera. Thin Black shale layers are interbedded with Buda Limestone. The bedding is highly burrow mottled and produced nodular bedding (modified after Zhang 2016)

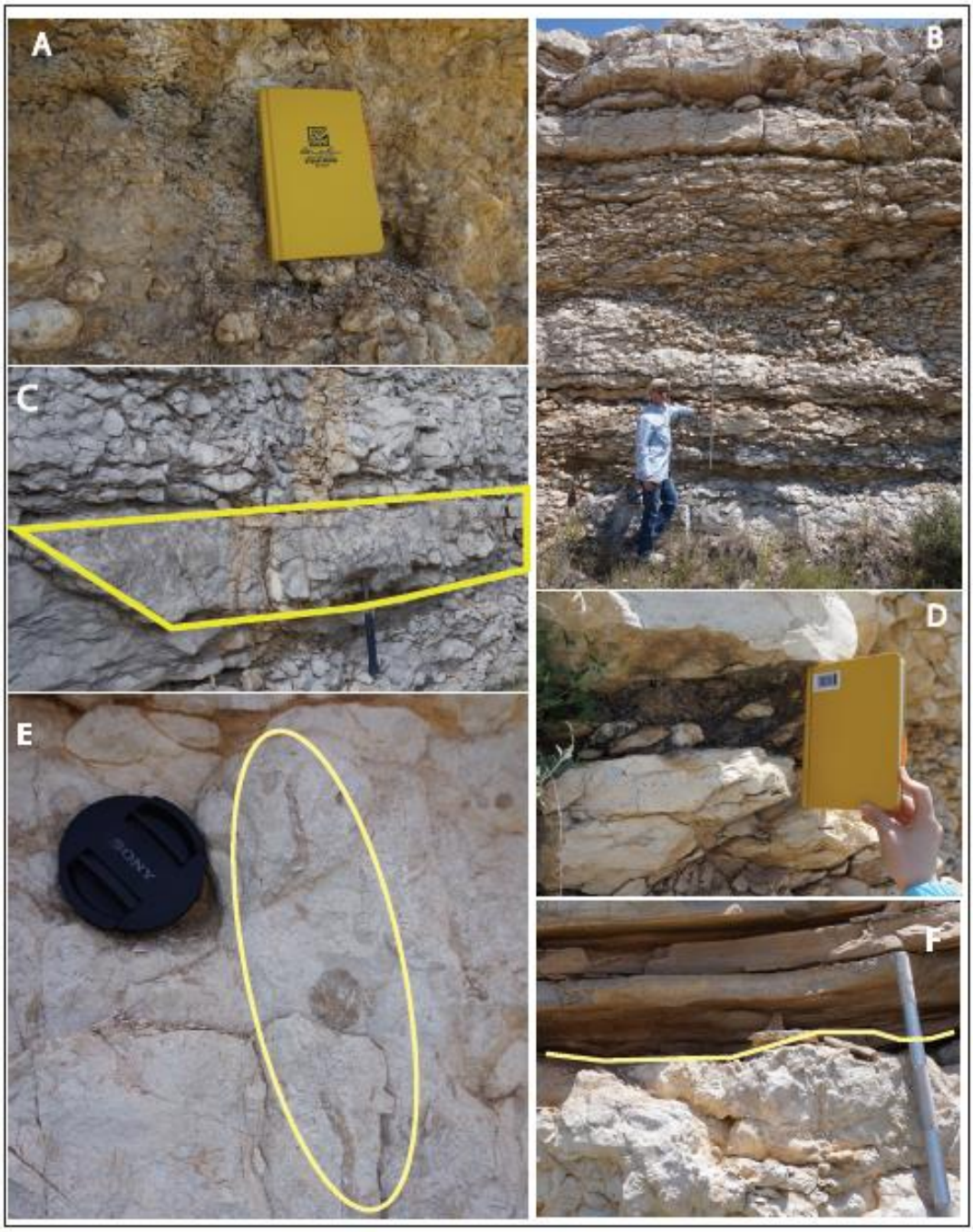

Figure 5. Typical Buda Formation outcrop features A. Buda and Del Rio unconformity contact with abundant clasts from Buda Formation. B. Nodular bedding produced bioturbation and differential cementation. C. Small channel filled with skeletal packstone facies 6 m above the Buda-Del Rio contact. D. Typical thin black shale layers interbedded with the limestone. E. Burrows (circled) in nodular bedding F. unconformable contact of Buda- Lower Eagle Ford formations.

constructed through central Texas: one cross section spans from Austin outcrop area to southeast corner of Lee county, and an other one from northwest San Antonio outcrop to northwest Karnes county, and the third one is oriented the San Marcos Arch (SMA) without any outcrop correlations. One strike cross-section is parallel to the paleo shelf margin across the whole study area.

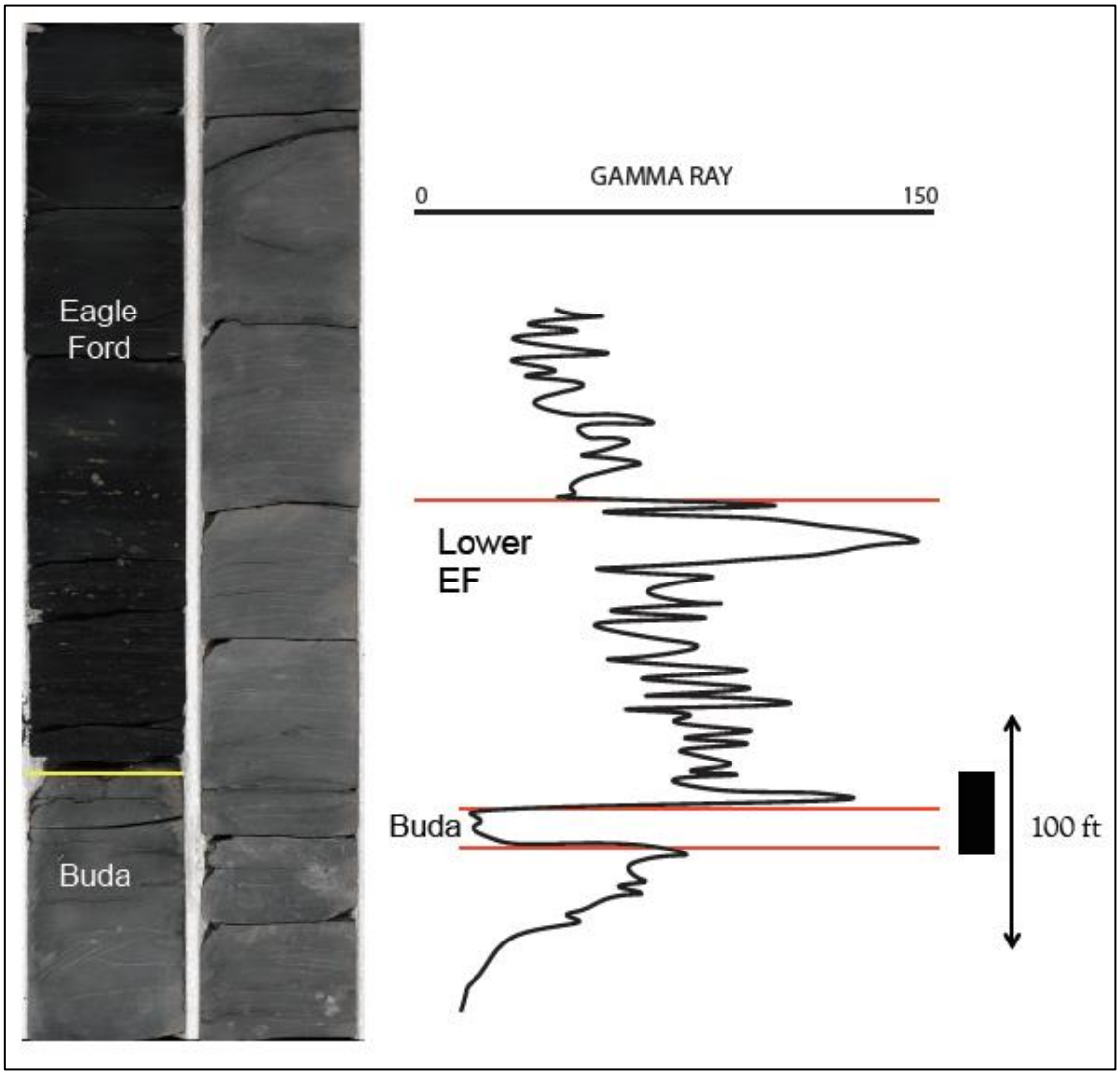

Figure 6. Typical GR profile of the Buda Formation with low GR values. Core from Karnes County shows sharp contact from Buda Formation to Lower Eagle Ford group.

CHAPTER V

RESULTS

Depositional Facies

Due to fossil variations and matrix content difference, three facies are interpreted (deepest to shallowest) from subtidal outer ramp foraminifera mudstone, inner ramp skeletal wackestone/packstone to lagoonal massive mudstone of Buda Formation based on outcrops in west Texas and cores in central Texas (Figure 7). Both cores show following two facies consistently with similar bedding structures.

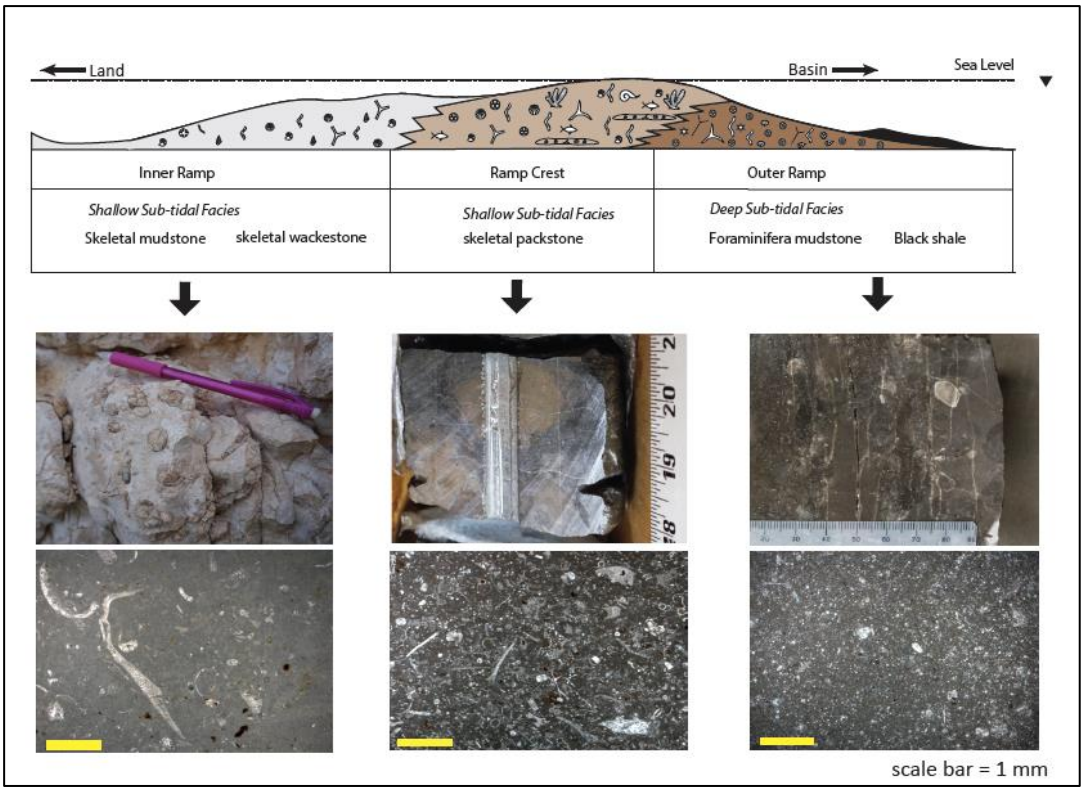

Figure 7. Facies interpretation of the Buda Formation outcrop to subsurface study, shows landward to basinward change along ramp profile. Inner ramp facies consist of massive skeletal mudstone and wackestone, ramp crest facies are skeletal packstone, and outer ramp facies are foraminifera mudstone and black shale. Inner ramp facies are most common updip at outcrop locality whereas ramp crest and outer ram facies are most common in subsurface portion of this study.

Massive Foramniferal Mudstone

Foraminifera mudstone facies generally has dark brownish color with thin shaly seams producing nodular bedding with high bioturbation index BI=3, (Taylor & Goldring, 1993). This facies is common toward the base of the core, with organic matter restricted the deeper part of the Buda Formation. The matrix is composed of abundant clay-sized foraminifera fossils with less than 10% shell fragments. Major planktonic fossils include globigerinid (*F. washitensis, G. bentonensis, Hedbergella, H. moremani, P. appenninica, Rotalipora*) (Plate 1). Large benthic foraminifera and nannofossils (calcisphere and dinoflagellates) are well distributed in the core as well (Figure 8). The depositional environment is interpreted as outer ramp subtidal shallow marine environment with water depth range from 50 to 100 feet (Jones, 2013). The water conditions were well oxygenated with low salinity as suggested by the abundance of large benthic forams and nannofossils. Outcrops in west Texas did not have this facies, but they contain abundant microfossil (calcisphere, algal fragments and sponge spicules) in the lagoonal mudstone facies.

Massive Skeletal Wackestone/Packstone

This facies occurred in both core and outcrop samples. The massive skeletal wackestone/packstone facies shown in the core has grayish white color compared to the dark gray foraminifera mudstone (Figure 8). There are more fossil fragments in the core than that of outcrop samples, but skeletal grain types are quite consistent. The major

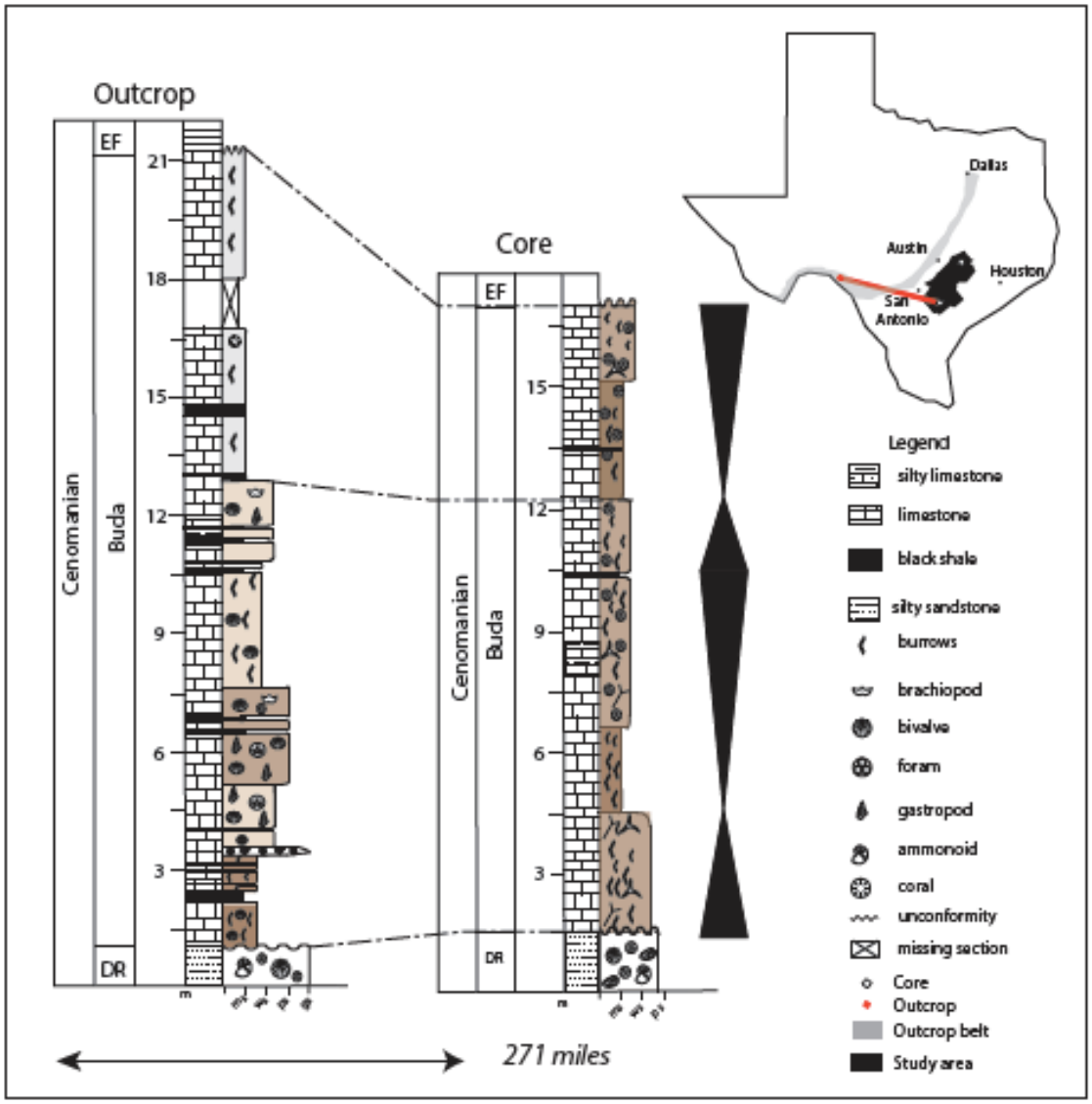

Figure 8. Subsurface core to outcrop correlation shows facies variation from massive mudstone to skeletal wackestone/packstone. Two depositional cycles interpreted from core description. One possible maximum flooding surface occurred in the Buda–False Buda transitional zone. Facies colors correspond to depositional profile from dark brown foraminifera mudstone to light grayish brown skeletal wackestone/packstone facies.

fossil types are sponge spicules, bivalves, gastropods, bryozoans, and fish bone debris. Skeletal wackestone/packstone bedding is highly bioturbated (up to BI=5). Abundant glauconite minerals are common in this facies as well. The Depositional environment of

this facies is interpreted as inner ramp intertidal to subtidal shallow marine with water depth less than 50 feet. Outcrops in west Texas also have similar facies features but with larger bivalve and gastropod fragments filling a small channel cut which indicate the depositional setting might be close to skeletal shoal barriers.

Compare to fragmental fossils in the core, outcrop samples have much larger complete skeletal grains. 6 and 12 meters above the Buda-Del Rio contact in the measured section of west Texas (Figure 4), there are two small channels (30 cm height with 3 m length) dominated with skeletal grainstone indicating the depositional setting might be once close to skeletal shoal barrier (Figure 7). Above the channel succession, massive skeletal wackestone/packstone contain interbedded thin black shale layers. Large (~2 cm) pelecypod and gastropod fragments are common in outcrops. Some oyster fragments are well preserved in the Del Rio and Buda contact interval (Figure 4). Outcrops in San Antonio area also contain large gastropod (~3 cm) and pelecypod fragments (~3 cm) preserved in the beddings. Outcrop in west and central Texas shows the Buda-Del Rio contact contain abundant rip-up clasts with borings at the base of Buda Formation.

Massive skeletal mudstone

This facies only occurred in outcrop samples from west Texas. The bedding in the outcrop is highly bioturbated (BI=6) with whitish gray color. Some large fossils like coral, gastropod, were common replaced by sparry calcite in the mud matrix.

Organic rich black shale layers are observed both in the outcrop and core, however in the core shale layers are mainly composed of foraminifera mudstone which is different from clay dominated outcrop shale layers (Figure 8).

Correlation

Three facies identified of Buda Formation based on core data combined with previous work (Zhang, 2016) in outcrop composed of inner ramp lagoonal massive mudstone/wackestone facies express a low relief ramp profile (Figure 7). Facies correlation from outcrop to core (Figure 8), shows shallowing upward depositional facies changes from relative deep subtidal foraminfera mudstone to intertidal skeletal wackestone/packstone up to lagoonal mudstone/wackestone. The massive mudstone facies bounded by shale flooding surfaces with increasing microfossil abundance compare to skeletal wackstone packstone facies.

Correlations of more than 150 wireline logs with one core control in Lee County are used for making thickness map and showing depositional geometry in the subsurface throughout central Texas area (Figure 2). The Buda Formation thickens toward the southwest into the Maverick basin and thins onto east side of the San Marcos Arch (Figure 9). The thickness ranges from 20 to 120 feet. Thickness is thinning significantly in Lee, Gonzales, and Dewitt counties but thickening up to 100 feet in Guadalupe, Caldwell and Gonzales counties of the study area based on wireline log correlation. Cross-section A-A' along the paleo-shelf margin in northeast to southwest direction (Figure 10) shows relatively uniform depositional geometry with variable thickness change from 80 to 120 feet. Dip cross-section B-B' perpendicular to the paleo-shelf

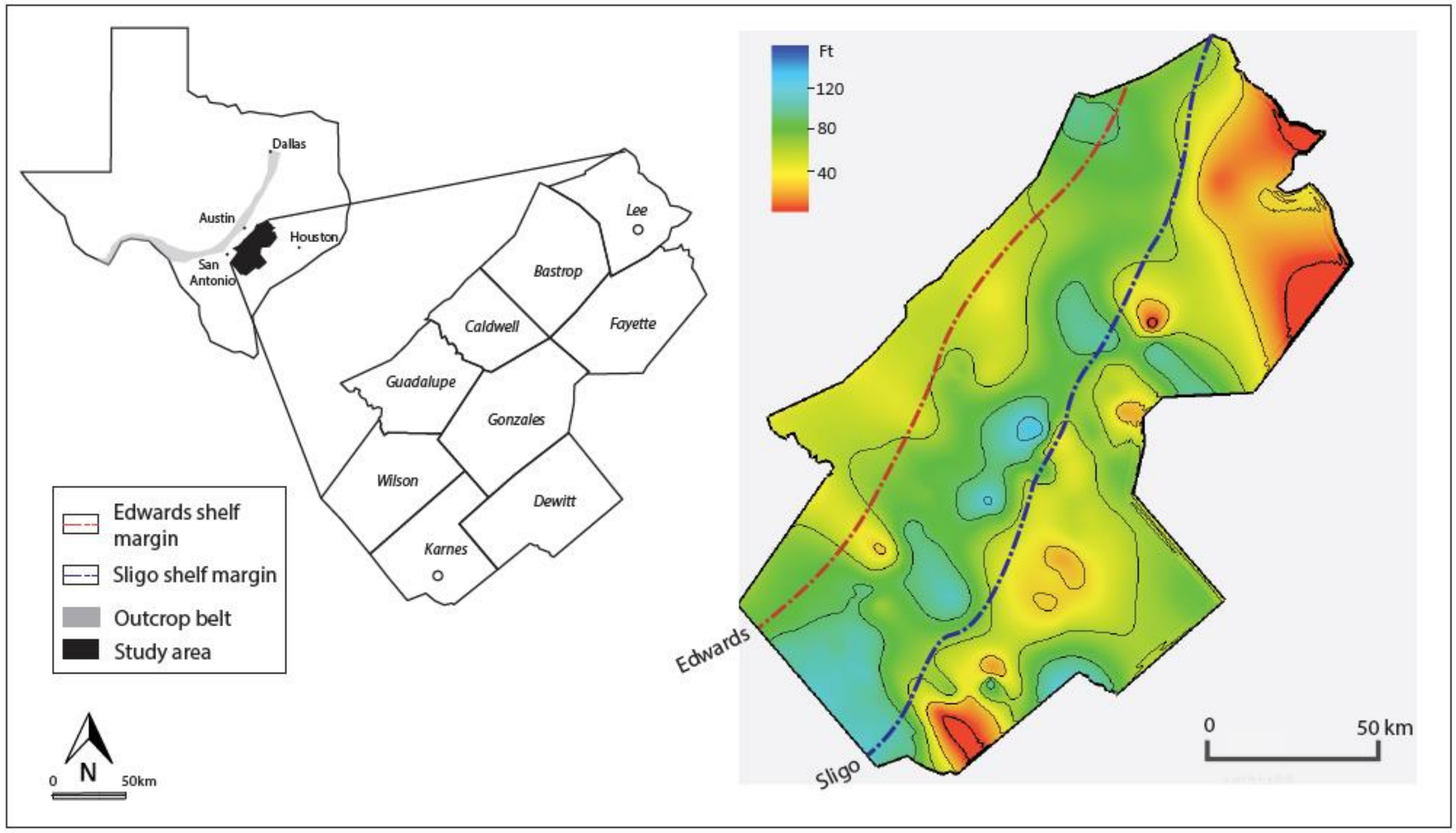

Figure 9. Isochore map of the Buda Formation in subsurface central Texas based on wireline log correlations. The thickness increases to the southwest toward Maverick basin area and decrease onto the San Marcos Arch to the east side of Gonzales, Fayette and Lee counties.

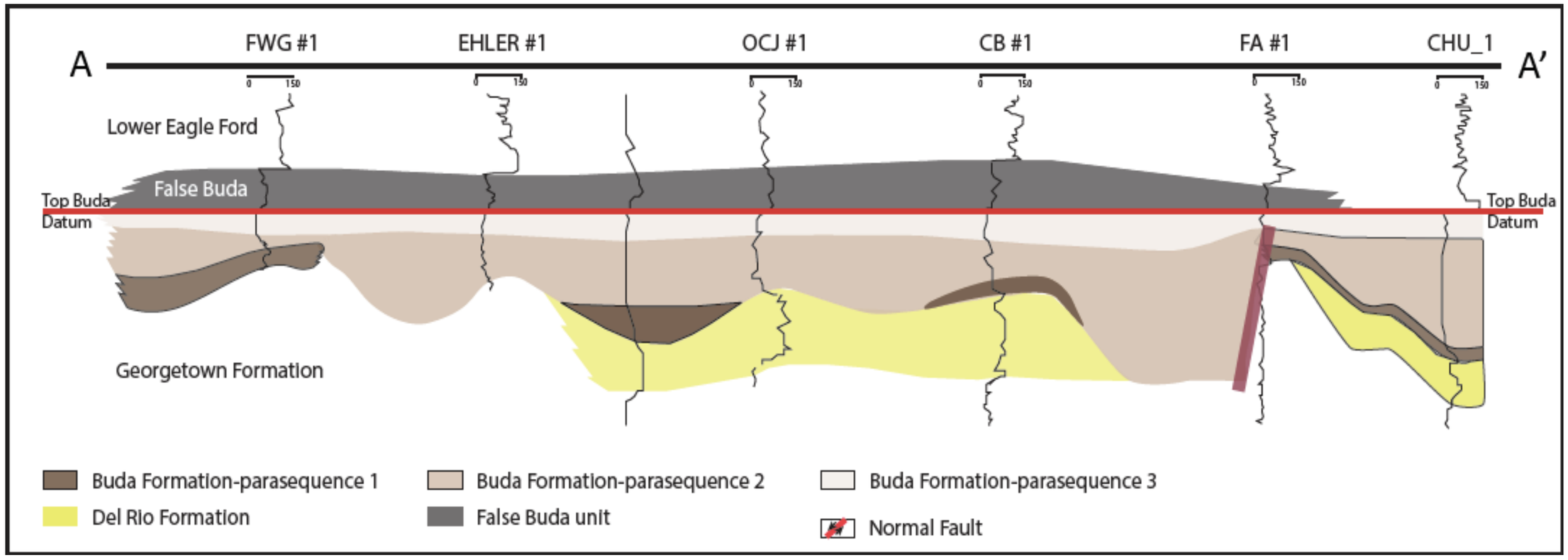

Figure 10. Cross section A-A' shows strike direction (parallel to the paleo shelf margin) wireline correlation of Lower Eagle Ford, False Buda, Buda, Del Rio Formation, and Georgetown Formations. There is relative uniform thickness of Buda parasequence 3 dominated by massive mudstone. The dark brownish foraminifera mudstone dominated parasequence 1 shows mosaic depositional geometries possibly due to syntectonic uplifts. Local fault structure is shown significant thickness changes of Buda Formation and Del Rio Formation.

margin reveals aggradational geometry with thickness change from 30 to 120 feet (Figure 11). Cross section C-C' (Figure 12) shows thinning of the Buda Formation right to the top of SMA. Between two paleo shelf margins (Edwards and Sligo) on the thickness map, a thickening trend extends southwest towards the Maverick basin area and may be the evidence of regional paleotopographic Karnes Trough across central Texas during Buda Formation deposition.

Three shallowing upward parasequences interpreted from wireline log patterns are corresponding to two flooding surface interpreted from facies correlation. Figure 10 indicates parasequences 2 dominated by skeletal wackestone/packstone has the thickest interval with high resistivity and porosity.

Geochemical results

Stable isotope

Figure 13 shows the relationship of $\delta^{13}C_{vPDB}$ and $\delta^{18}O_{vPDB}$ with depth and rock facies from core in Lee County. $\delta^{13}C_{vPDB}$ of Buda Formation ranges from +0.5 ‰ to +2.5‰, and $\delta^{18}O_{vPDB}$ varies from -7 ‰ to -2.5 ‰. Near the Del Rio-Buda Formation contact about 3.28 ft (1 m) above the Del Rio in the core, a positive excursion occurs from +1.5 to +2.1 ‰ of $\delta^{13}C_{vPDB}$. In the Buda Formation, one positive excursion occurs around 9.8 ft (3 m) above the Del Rio with a 0.2‰ increase from +1.7 to +1.9‰ of $\delta^{13}C_{vPDB}$. 26.2 ft (8 m) above the Del Rio in the Buda-False Buda transition zone, $\delta^{13}C_{vPDB}$ increases 0.8 ‰ and $\delta^{18}O_{vPDB}$ ranges from -5.1 to -2.7‰ within 6.5 ft (2 m) interval. One large negative excursion of δ^{13}CvPDB from +1.00 ‰ to -1.25 ‰ with

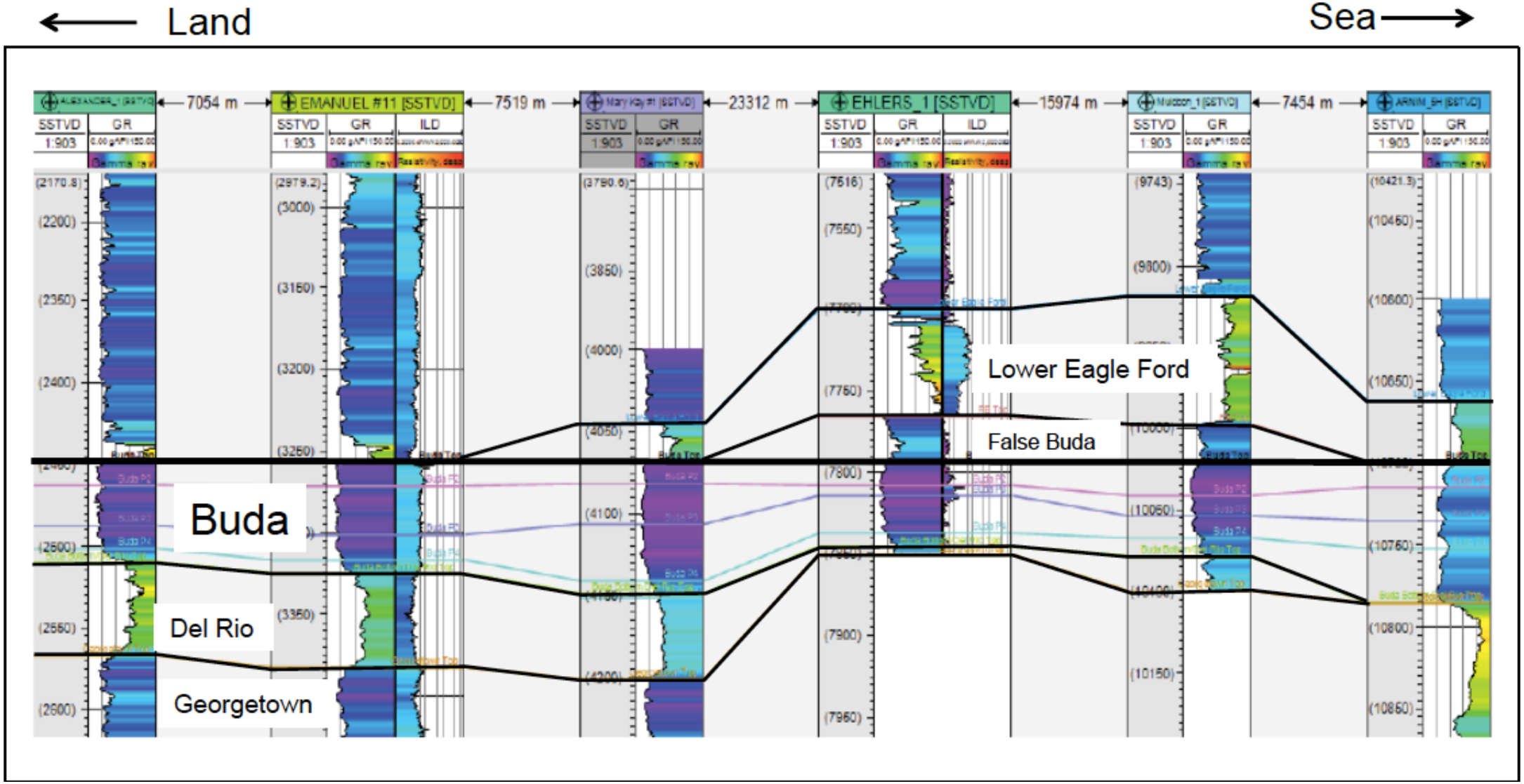

Figure 11. B-B' Dip direction correlation of Buda Formation in eastern part of study area. The False Buda unit is thinning into the Sligo shelf margin, whilst the Lower Eagle Ford formation is thickening toward the basin side. Buda shows a progradational migration of the thickness into the Sligo shelf margin. Color lines represent flooding surfaces occurred in Buda Formation

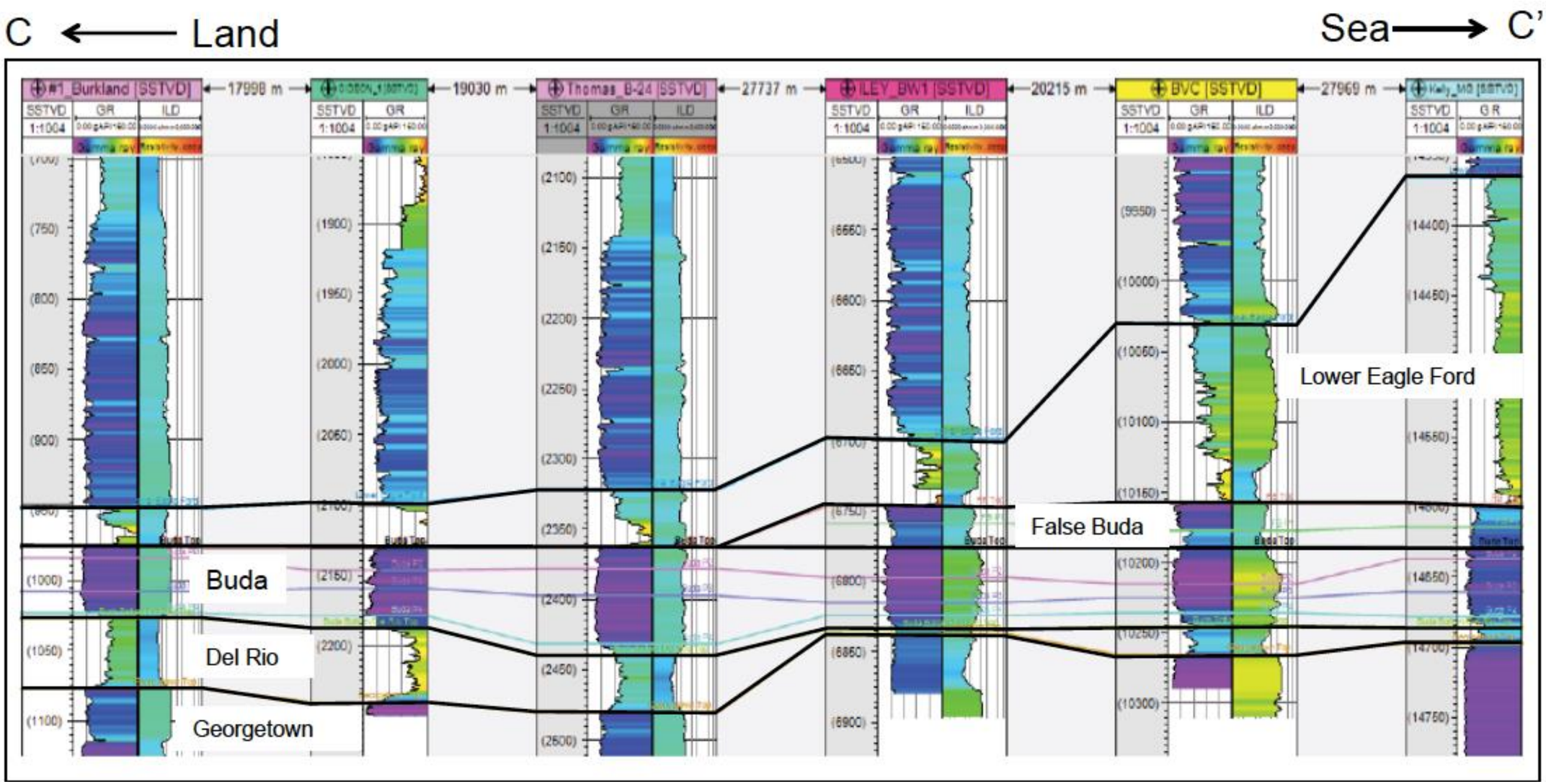

Figure 12. C-C' correlation show the thickness of Buda Formation is thinning onto the San Marcos Arch compared to B-B' correlation. Color lines represent flooding surfaces occurred in the Buda Formation.

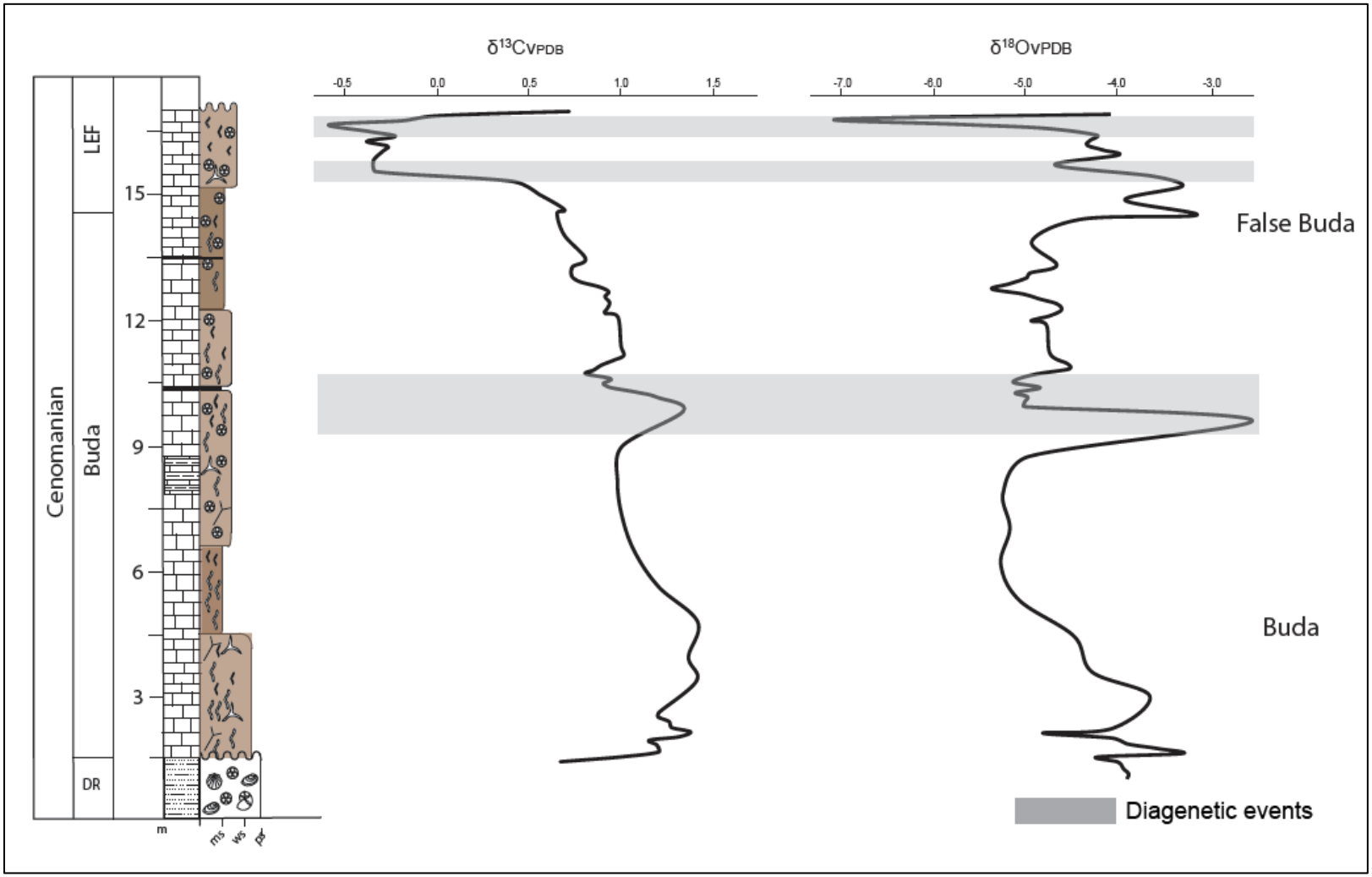

Figure 13. Stable isotope profile of Buda Formation from Lee core in central Texas. Large negative excursion occurs the False Buda-Buda Formation transition zone. $\delta 13C_{VPDB}$ of Buda Formation ranges from +0.5 ‰ to +2.5‰, and $\delta 18O_{VPDB}$ varies from -7 ‰ to -2.5 ‰.

$\delta^{18}O_{vPDB}$ from -4.2 to -6.8 ‰ occurs around 52.5 ft (16 m) above Del Rio in the core, which corresponds with the transition zone from the "False Buda" unit to Lower Eagle Ford Formation. The isotopic values delineate a reversed "J" pattern on a $\delta^{13}C_{vPDB}$ vs. $\delta^{18}O_{vPDB}$ cross plot (Figure 14).

Cathodoluminescence (CL)

Two core samples LB_19 and KB_2 with skeletal grains replaced by sparry calcite cements were analyzed with cathodoluminescence. One large bivalve fragment is focused on detecting luminescence of LB_19 sample that is dominated with massive skeletal packstone. KB_2 sample is massive mudstone with abundant neomorphic blocky sparry calcite cements in fractures. Two luminescence stages occur in both samples including dull/black and bright orange (Figure 15). LB_19 has dull luminescence of lime mud matrix with two different color of cements bright yellow and dull color. Two stages luminescence of the cements in LB_19 indicates probably two diagenetic events occurring synchronous calcite crystal growth in the primary pore space (dull) and secondary cementation (bright orange). KB_2 has primary cementation with dull color as the mud matrix and bright orange color for the rest of the skeletal grain. Dolomitization occurred in the KB_2 cements with rhombic crystal feature in bright orange color within the dull marine cements.

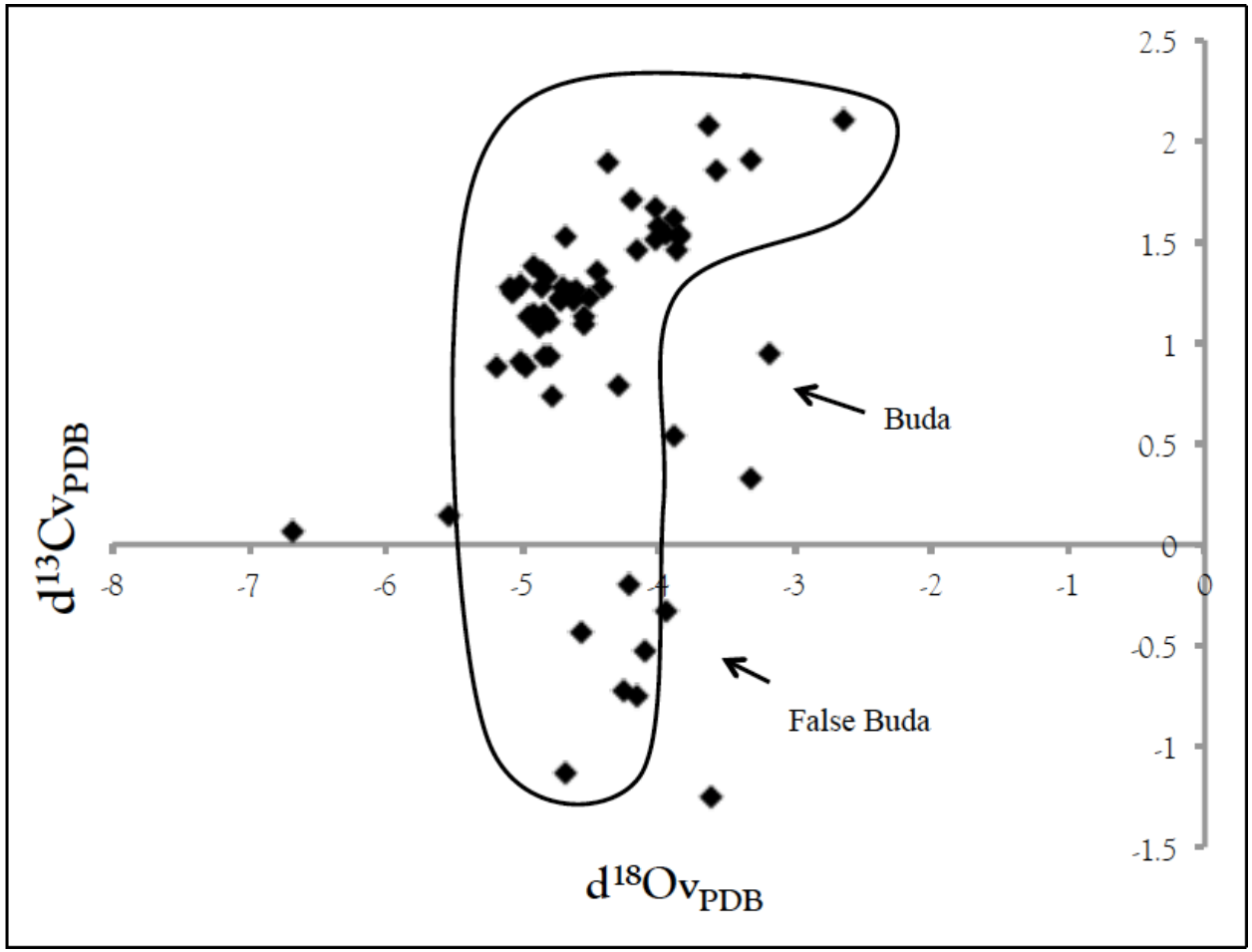

Figure 14. Cross plot of relationship between $\delta^{13}Cv_{PDB}$ and $\delta^{18}O_{vPDB}$ shows a reversed "J" pattern in Lee County whole-rock core samples. Negative $\delta^{13}Cv_{PDB}$ samples from False Buda unit.

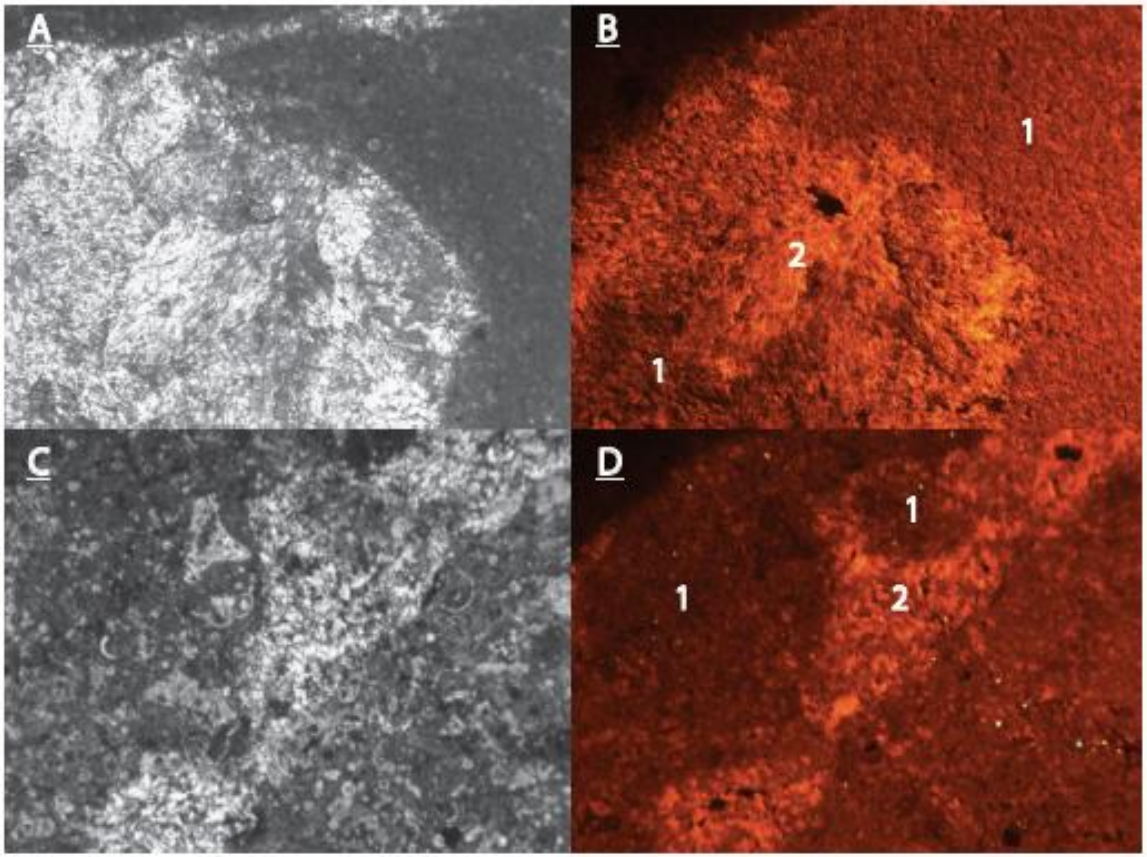

Figure 15. CL images of LB_19 (A&B) and KB_2 (C&D) from Lee County core and Karnes County core. A. Photomicrograph of LB 19 shows sparry calcite cements replaced skeletal grains. B. CL image of LB_19 show two luminescence stages 1 and 2 from dull to bright yellow colors. C. Photomicrograph of KB_2 is bivalve fragment replaced by calcite cements. D. CL image of KB_2 cement with primary dull color matrix to fresh water cementation with bright yellow color.

CHAPTER VI

DISCUSSION

Stratigraphy

Previous work (Ak 2015, Erdogan 1969, Martin 1968) suggests Buda Formation has two facies types based on fossil assemblage: shallow water skeletal wackestone facies and deeper water facies with foraminifera in central Texas. The deposition environment of Buda Formation found in a low energy, open marine shallow water setting (Brown 1981). In this study, two facies interpreted from subtidal inner ramp to outer ramp possibly across ramp crest in the shallow marine water. The size of fossils and abundance of shell fragments increase toward shallower water (Hudson 1977), and the relative fossil size in the Buda Formation indicate the shallowest depositional environment is in outcrops of west Texas, and the deepest was in core from central Texas. Fossil variations of the Buda Formation from macrofossil to microfossil indicate water conditions changed slightly. Top 3-meter (12 feet) interval of Buda Formation in the outcrop of west Texas shows abundant large skeletal grains (including gastropod, inoceramid, coral, and sponge spicules) imply a skeletal barrier in the inner ramp shallow marine environment with abundant fish debris. Two small channels (3 m by 5 m) dominated with skeletal grainstone indicate ramp crest possibly produced in place for a short period. The planktonic foraminifera assemblage in the Buda Formation is exclusively composed of *globigerinids* a genus that dwelled in shallow epipelagic to mesopelagic environments (Jones 2006). The major planktonic marker *Favusella. Washitensis* (*F. Washitensis*) that is the most abundant species in the Buda Formation is

used to separate Buda and Eagle Ford or Woodbine Formations. Another dominant *Hedbergella* species interpreted as surface dwelling condition appears tolerant of less than normal marine salinity that suggesting the Buda Formation was even possibly deposited in a brackish water with freshwater input into shallow marine setting. The enriched $\delta^{13}C$ signatures of some surface-dwelling taxa provide evidence of photosymbiosis (Jones 2006). Core located in the Lee County shows high-enriched ^{13}C values (Figure 13) in the deeper interval of Buda Formation according to stable isotope data ($\delta^{13}C_{vPDB}$ from 0.5 to +2.5‰). Algal fragments and bryozoan pieces are common in the foramniferal dominated wackestone, suggesting the planktonic foram was probably living symbiotically with algae/bryozoan within the photic zone in well-oxygenated shallow water column. High bioturbation index with nodular bedding in the core and outcrops delineates the depositional setting was probably above fair weather base up to open marine settings**.**

Figure 16 shows GR data correlated with major element compositions of the Buda Formation. About a 25 feet interval occurring above the Buda Formation was interpreted as False Buda Formation in the Lee County core. Previous research proposed that in central Texas (e.g. Gonzales, Karnes, Dewitt Counties), the False Buda is interpreted to be equivalent to the Maness Shale that is generally correlated to the base Lower Eagle Ford in south Texas (Denne & Breyer, 2016) Hentz, and Ruppel 2010;(Zumberge, Illich, & Waite, 2016). The petrography and geochemical analysis of the False Buda unit in this study indicates different rock textures and composition from the Buda Formation,

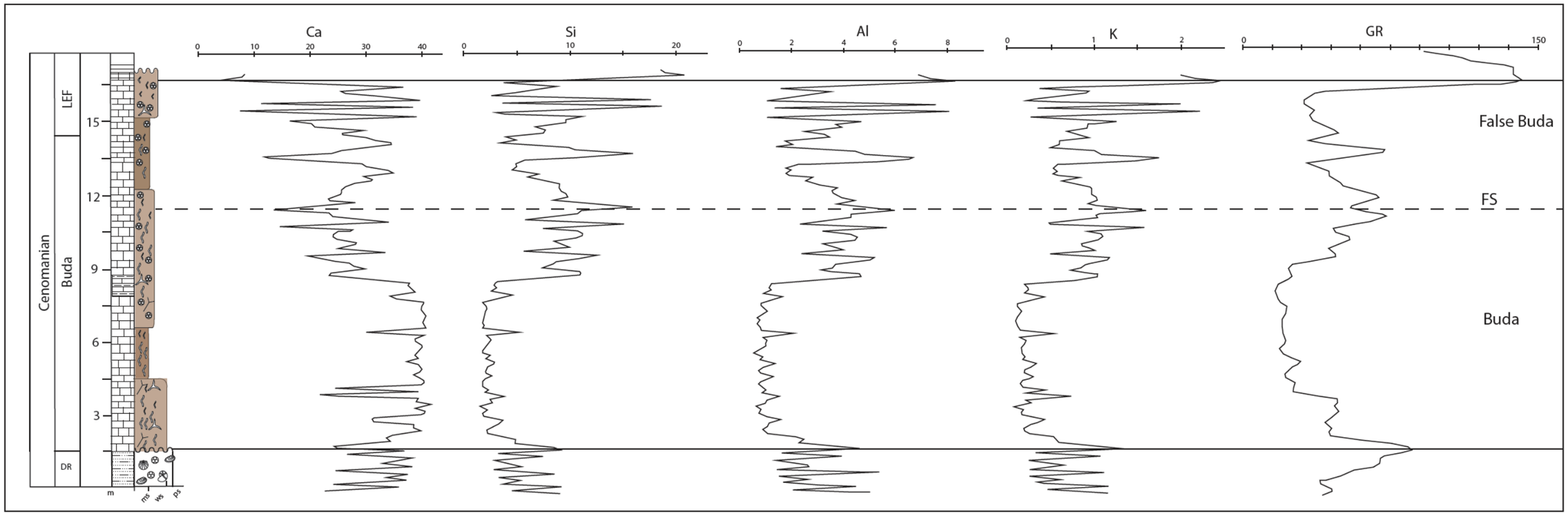

Figure 16. Geochemical analysis of Buda Formation showing compositions of Ca, Si, Al and K plotted against the total Gammy ray values. The False Buda unit shows similar low Calcium (<10%), high aluminum (5~10%) and silica (~15%) concentration with relative high GR values than the underlying Buda Formation. Dash line represent one possible flooding surface occurred during Buda Formation deposition.

consistent with previous work. The GR and major elements composition profiles are consistent with a sharp change from upper Buda interval to the False Buda unit. Relatively high GR values with low calcium but high silica composition of False Buda unit is quite different from the underlying Buda Formation. Compared to Lower Eagle Ford/Maness shale in central Texas (Denne et al. 2016), the False Buda shows similar low calcium (<10%), high aluminum (5~10%) and silica (~15%) concentrations with relative higher GR values than the underlying Buda Formation. The False Buda facies is dominated by a planktonic foraminifera enriched mudstone with rare benthic forams. More organic matter (possible hydrocarbons) was preserved in the False Buda than in the Buda Formation.

Unfilled accommodation space produced by paleotopography of the Sligo shelf margin was possibly filled during deposition of the Buda Formation or the overlying Eagle Ford Group (Phelps et al. 2014). Comparing the isochore map (Figure 17) of Buda Formation and False Buda unit, the accommodation space was filled balanced in the study area. As False Buda unit increases thickness, there was either no Buda Formation deposited or it was thinner. This depositional pattern is probably caused by paleotopographic features occurred during Late Cenomanian. This interchangeable thickness variation significantly expresses in the dip correlations that a discontinuous transgressive stacking pattern of the False Buda unit is on the top of the Buda Formation. The depositional geometry indicates the Buda Formation and False Buda unit are not in the same depositional cycle. This shaly argillaceous False Buda unit is highly possible

part of the Lower Eagle Ford sequence locally conformably overlying the Buda Formation based on subsurface correlations in central Texas.

Diagenesis

Two paragenetic events were recorded within the Buda Formation. One stage is the early marine cementation, where synchronous calcite cements show similar luminescence of the matrix indicating formative water in the pore space similar to the water condition in the ocean. The second stage is burial diagenesis, where blocky cements with some rhombic dolomite in cores with bright luminescence possibly show the meteoric or fresh water conditions under burial compaction deposition.

Several large negative excursions on the stable isotope profiles indicate possible subaerial exposure events occurred near the Del Rio Formation and Buda Formation contact and False Buda –Lower Eagle Ford group contacts.

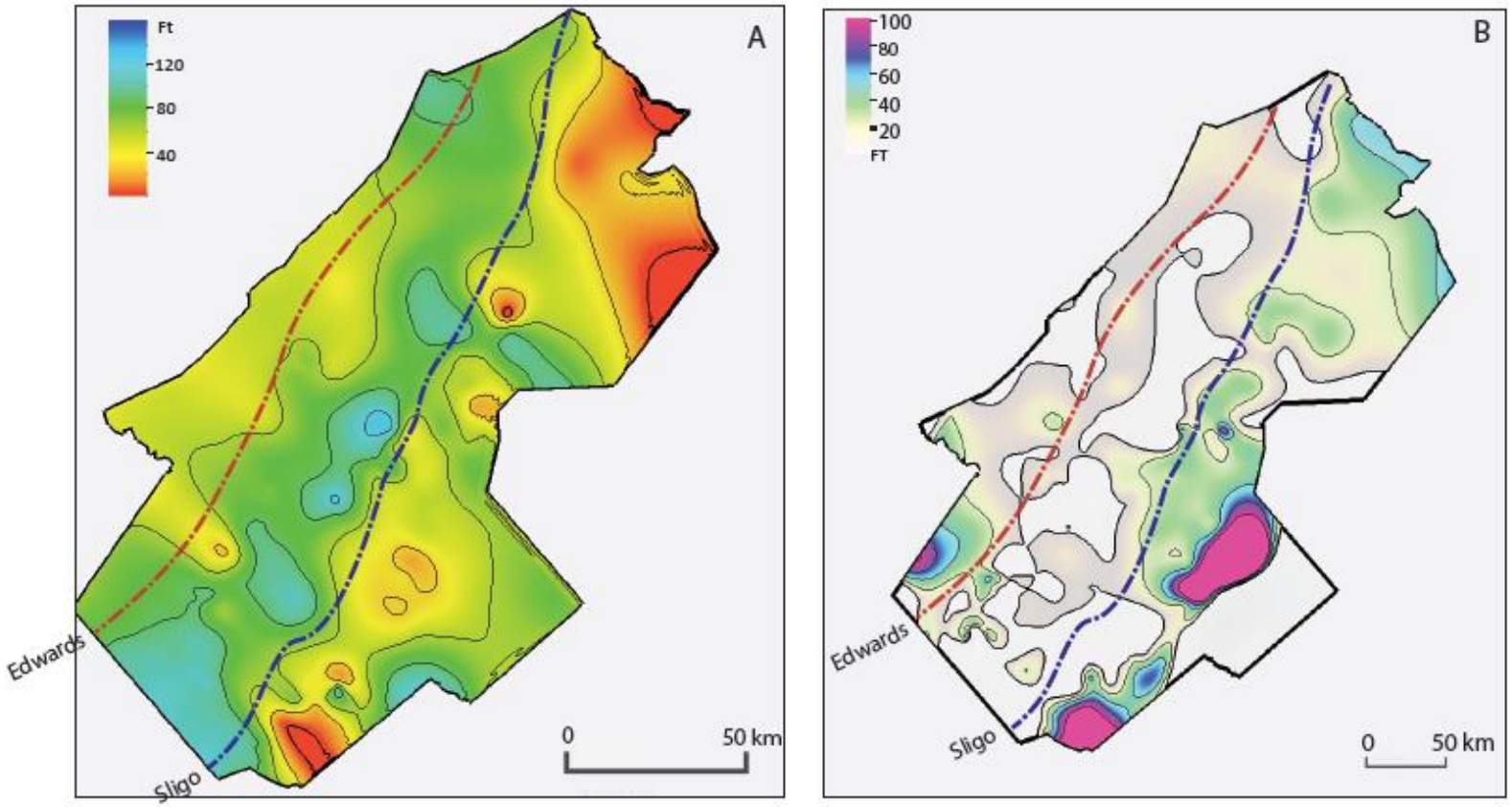

Figure 17. Comparison of isochore maps of Buda Formation and False Buda unit **A.** Thickness map of Buda Formation in central Texas based on wireline logs correlation. **B**. Thickness map of False Buda unit in central Texas. As False Buda unit increases thickness, there was either no Buda Formation deposited or it was thinner

CHAPTER VII

CONCLUSION

The Buda Formation records three distinguishable facies from deep subtidal outer ramp foraminfera mudstone to inner ramp skeletal wackestone/packstone in shallow marine depositional environments. Major fossil groups are bivalve (pelecypod), gastropod, bryozoan, and sponge spicules. Microfossils are mainly dominated with planktonic forams *globigerinid (F. washitensis, G. bentonensis, Hedbergella, H. moremani, P. appenninica, Rotalipora)*, large benthic foraminifera and nannofossils (calcisphere and dinoflagellates). The water condition was well oxygenated during deposition with low salinity as suggested by the abundance of large benthic forams. Highly bioturbated bedding with nodular structures both in outcrop and core explains the high tide dominated open marine shallow water environment.

Surface to subsurface correlations across the study area shows the Buda Formation was deposited from the outcrop belt to the subsurface with quite uniform thickness along paleo shelf margins direction. Dip direction (perpendicular to paleo shelf margin) reveals the aggradational stacking patterns of the Buda Formation toward paleo Gulf Mexico basin side. Stratigraphically the False Buda unit is conformable above the Buda Formation in central Texas and ranges from 20 to 80 feet in thickness. Its chemical composition more similar to the lower Eagle Ford indicate the False Buda unit was deposited in a separate depositional cycle correlative with the basal part of the Lower Eagle Ford Formation.

The Buda Formation records two paragenetic phases. One stage is early marine cementation, and second stage is burial diagenesis. The Buda Formation has abundant blocky calcite cements with rhombic dolomite found during burial compaction. Boring structures in the outcrops of Del Rio-Buda contact with negative excursion in the $\delta^{13}C_{vPDB}$ profile appears the subaerial exposure in west Texas. Similar features are shown in the core stable isotope data that large negative excursion near False Buda-Lower Eagle Ford transition zone with enriched ^{12}C of the False Buda unit means possibly subaerial exposure or submarine erosion.

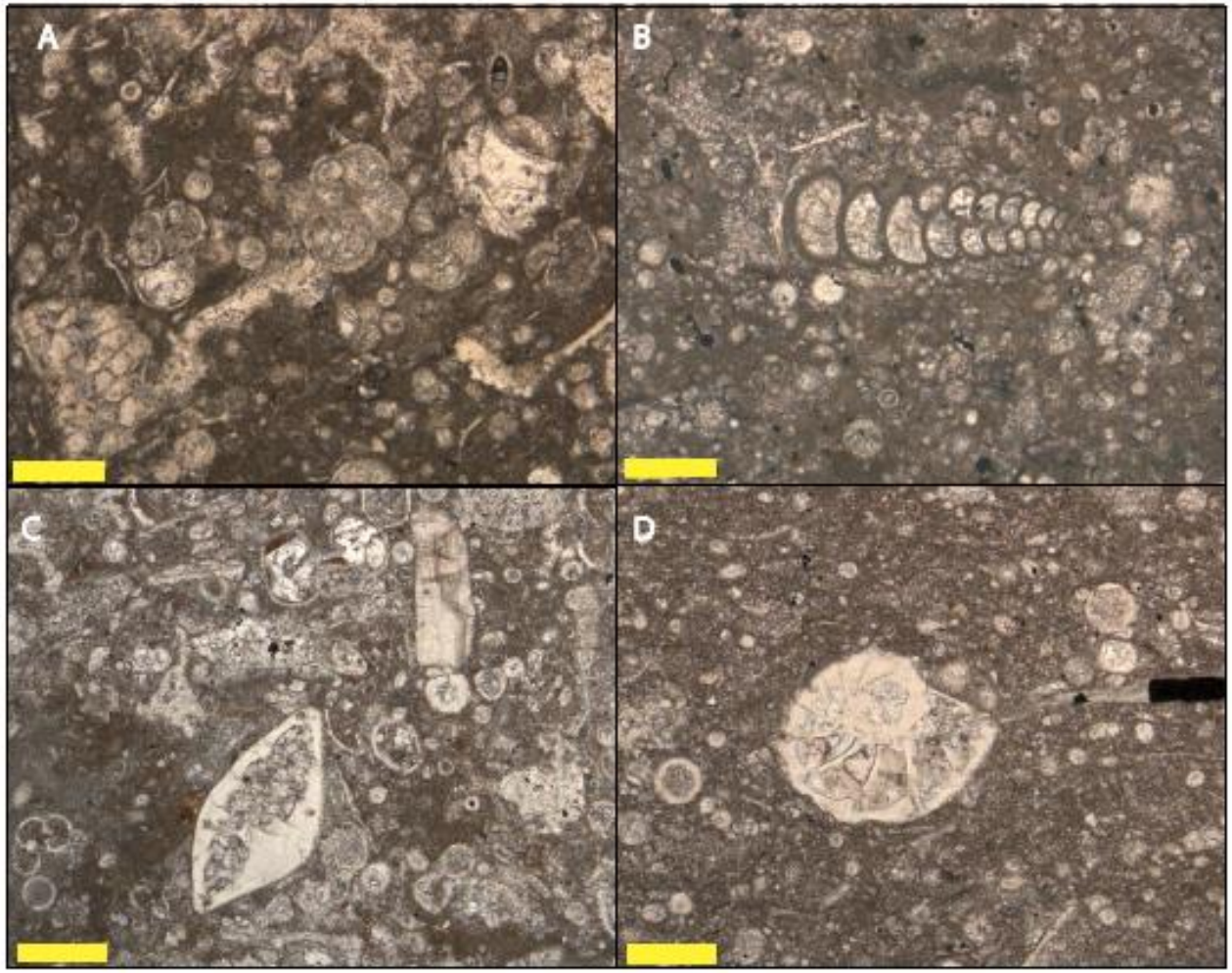

Plate 1. Common foraminifera species occurred in the Buda Formation. A. *F. washitensis* B. *Hedbergella* C &D. Large benthic forams (Scale bar=0.2mm).

REFERENCES

Ak, O. (2015). *The depositional environment and the diagenetic processes of the buda limestone (Cenomanian) in south-central Texas.* THE UNIVERSITY OF TEXAS AT SAN ANTONIO.

Boggs, S., & Krinsley, D. (2006). Applications of CL Imaging to the Study of Sedimentary Rocks: Cambridge University Press, New York.

Brown, T. (1971). Stratigraphy of the Washita Group in Central Texas: Baylor Geol. *Studies Bull, 21*, 43.

Culotta, R., Latham, T., Sydow, M., Oliver, J., Brown, L., & Kaufman, S. (1992). Deep Structure of the Texas Gulf Passive Margin and its Ouachita-Precambrian Basement: Results of the COCORP San Marcos Arch Survey (1). *AAPG Bulletin, 76*(2), 270-283.

Denne, R. A., & Breyer, J. A. (2016). Regional Depositional Episodes of the Cenomanian–Turonian Eagle Ford and Woodbine Groups of Texas. *AAPG Memoir, 110*, 87-133. doi:10.1306/13541959m1103660

Dickey, R. L. (1983). *The stratigraphy and petroleum potential of the Buda Limestone (Cretaceous) in Central Texas.* (Bachelor thesis), Baylor University, Waco.

Erdogan, S. Z. (1969). *Microbiofacies of the Cenomanian Buda Limestone (Comanche Cretaceous) and Trans-Pecos Texas.* (Master), Louisiana State University

Fairbanks, M. D., Ruppel, S. C., & Rowe, H. (2016). High-resolution stratigraphy and facies architecture of the Upper Cretaceous (Cenomanian–Turonian) Eagle Ford

Group, Central Texas. *AAPG Bulletin, 100*(03), 379-403. doi:10.1306/12071514187

Haq, B. U. (2014). Cretaceous eustasy revisited. *Global and Planetary Change, 113*, 44-58.

Hentz, T. F., & Ruppel, S. C. (2010). Regional lithostratigraphy of the Eagle Ford Shale: Maverick Basin to East Texas Basin. *Gulf Coast Association of Geological Societies Transactions, 60*, 325-337.

Horstmann, L. E. (1987). Giddings Field: Bastrop, Brazos, Burleson, Fayette, Lee, and Washinton Counties. *Houston Geological Society, 2*, 217-233.

Hover, V. C., Bases, F. S., & and Lock, B. E. (2008). Clay Mineralogy of the Del Rio Clay Formation (Cenomanian), West Texas: Illite/Kaolinite Ratios as Relative Salinity Indicators.

Jones, R. W. (2013). *Foraminifera and their Applications*: Cambridge University Press.

Lock, B. E., Grimball, J. W., & Johnson, J. G. (2013). The Cenomanian Del Rio Formation in West Texas.

Luttrell, P. E. (1977). Carbonate facies distribution and diagenesis associated with volcanic cones-Anacacho Limestone (Upper Cretaceous) Elaine Field, Dimmit County, Texas. *Gulf Coast Association of Geological Societies Transactions, 27*, 441-442.

Mancini. (1977). Depositional environment of the Grayson Formation (Upper Cretaceous) of Texas.

Mancini, E. A., Obid, J., Badali, M., Liu, K., & and Parcell, W. C. (2008). Sequence-stratigraphic analysis of Jurassic and Cretaceous strata and petroleum exploration in the central and eastern Gulf coastal plain, United States. *AAPG Bulletin, 92*(12), 1655-1686.

Martin, K. G. (1961). *Washita group stratigraphy south-central Texas.* (Master), The University of Texas Austin.

Montgomery, S. L. (1990). Horizontal drilling in the Austin Chalk; Part 1, Geology, Drilling history and field rules. *Petroleum Frontiers, 7*, 44.

Phelps, R. M. (2011). *Middle-Hauterivian to Lower-Campanian sequence stratigraphy and stable isotope geochemistry of the Comanche platform, south Texas.*

Phelps, R. M., Kerans, C., Loucks, R. G., Da Gama, R. O., Jeremiah, J., & Hull, D. (2014). Oceanographic and eustatic control of carbonate platform evolution and sequence stratigraphy on the Cretaceous (Valanginian–Campanian) passive margin, northern Gulf of Mexico. *Sedimentology, 61*(2), 461-496.

Reaser, D., & Dawson, W. (1995). Geologic Study of Upper Cretaceous (Cenomanian) Buda Limestone Outliers in Northeast Texas. *TRANSACTIONS-GULF COAST ASSOCIATION OF GEOLOGICAL SOCIETIES*, 495-502.

Scott, R. W., Benson, D. G., Morin, R. W., Shaffer, B. L., & and Oboh-Ikuenobe, F. E. (2003). *Integrated Albian-lower Cenomanian chronostratigraphy standard, Trinity River section, Texas.* Paper presented at the US Gulf Coast Cretaceous stratigraphy and paleoecology: Gulf Coast Section, Society of Economic Paleontologists and Mineralogists, Bob F. Perkins Memorial Conference.

Sohl, N. F., E. Martinez, P. Salmercon-Urrena, and F. Soto-Jaramillo. (1991). Upper Cretaceous in a Salvador, ed., The Gulf of Mexico Basin: The geology of North America. *Geological Society of America,*, 205-244.

Taylor, A. M., & Goldring, a. R. (1993). Description and analysis of bioturbation and ichnofabric. *Journal of the Geological Society, 150*(1), 141-148. doi:10.1144/gsjgs.150.1.0141

Turner, G. L. (1950). Chilton Field, Falls County, Texas. *Houston Geological Society*, 84-85.

Young, K. (1967). Comanche Series (Cretaceous), south central Texas. *Comanchean (Lower Cretaceous) Stratigraphy and Paleontology of Texas. Permian Basin Section, Society of Economic Paleontologists and Mineralogists, Publication, 67*, 9-29.

Young, K. (1986). Cretaceous, marine inundations of the San Marcos platform, Texas. *Cretaceous Research, 7*(2), 117-140.

Zhang, X., and M.C. Pope. (2016). Surface to subsurface stratigraphy of the Upper Cretaceous Buda Formation in west Texas. *Gulf Coast Association of Geological Societies Transactions, 66,* 1087.

Zink, E. R. (1957). Resume of the lower Cretaceous of South Texas. *Gulf Coast Association of Geological Societies Transactions, 7,* 13-22.

Zumberge, J., Illich, H., & Waite, L. (2016). Petroleum Geochemistry of the Cenomanian–Turonian Eagle Ford Oils of South Texas. *AAPG Memoir, 110*, 135-165. doi:10.1306/13541960m110449

APPENDIX A

WIRELINE LOG DATABASE

API	County	Well name	Surf Lat	Surf Lon
4202130917	BASTROP	MCDONALD #12	30.096162	-97.465453
4202130919	BASTROP	ALEXANDER # 1	30.068039	-97.460155
4202130920	BASTROP	EMANUEL #11	30.050278	-97.389764
4202131088	BASTROP	F. D. BINGHAM #1	30.206218	-97.087018
4202131393	BASTROP	SHARP #1	29.993350	-97.526320
4202130913	BASTROP	Mary Kay #1	30.001278	-97.335655
4202131093	BASTROP	MCARTHUR #1	30.104471	-97.227036
4205532414	CALDWELL	Bairs 1-D	29.694035	-97.665219
4205532869	CALDWELL	CIDEON #1	29.777081	-97.719383
4205533954	CALDWELL	L.D #2	29.897387	-97.646583
4205534042	CALDWELL	A. J. #7B	29.914503	-97.540935
4205534144	CALDWELL	#1 Burkland	29.921661	-97.80490
4205534462	CALDWELL	A. W. JOLLEY#8	29.896032	-97.731851
4205534497	CALDWELL	STROMBERG #1	30.015336	-97.686812
4205534746	CALDWELL	N. K. O #1	29.979467	-97.705216
4205534778	CALDWELL	M.M #33	29.712913	-97.739737
4205533690	CALDWELL	M. B-33A	29.738832	-97.615989
4212331813	DEWITT	Blackwell_2	28.911973	-97.663704
4212332090	DEWITT	Cowtlow_Gas_1	29.087200	-97.375912
4212332229	DEWITT	Blackwell_gas_2	28.918901	-97.642296

4212331887	DEWITT	Boothe_1	29.130941	-98.200234
4212331713	DEWITT	Fort Worth_bank	29.05837	-97.47275
4212332226	DEWITT	Kelly_MG	29.1399	-97.26128
4212331198	DEWITT	KRAUSE	29.182577	-97.47486
4212332098	DEWITT	MENN_GAS_1	29.009521	-97.53803
4212331162	DEWITT	MILLER_1	29.214651	-97.45434
4212331793	DEWITT	RED_TRUST_1	29.040771	-97.44882
4212332014	DEWITT	WAGNER_2H	28.940174	-97.59295
4214933250	FAYATTE	ARNIM_5H	29.729225	-97.07461
4214932134	FAYATTE	EHLERS_1	29.927086	-97.10917
4214931825	FAYATTE	EPHESIENS_1	29.766348	-97.156784
4214932089	FAYATTE	GERALINE_1	29.916826	-97.085815
4214930482	FAYATTE	KOCIAN_1	29.815203	-97.16936
4214931708	FAYATTE	MILTON_1	29.971334	-96.80619
4214930476	FAYATTE	Muldoon_1	29.79268	-97.04869
4217731794	GONZALES	CB#1	29.364294	-97.66255
4217730798	GONZALES	RB#1	29.7636622	-97.3547114
4217731597	GONZALES	HTJ#1	29.3341371	-97.3782911
4217732242	GONZALES	ABG#1	29.595448	-97.26687
4217731707	GONZALES	MG#1	29.2813904	-97.4143769
4217731965	GONZALES	DA#4	29.2320671	-97.564996
4217731451	GONZALES	LEST#1	29.411976	-97.5
4217731382	GONZALES	WELLS_#1	29.477436	-97.4419

4217731803	GONZALES	EG#1	29.42119	-97.43322
4217731946	GONZALES	BB#1	29.464619	-97.29602
4217731639	GONZALES	Crozier#1	29.604866	-97.40718
4217730397	GONZALES	BCB	29.330969	-97.667061
4217730424	GONZALES	JM_DUBOSE1	29.557745	-97.341606
4217730525	GONZALES	OGSTON_SUSIE1	29.550888	-97.245255
4217730534	GONZALES	HOSKINS1	29.584799	-97.368713
4217730548	GONZALES	SPENCER_UNIT1	29.547113	-97.351028
4217730575	GONZALES	CINDY_B_UNIT1	29.497152	-97.283539
4217730599	GONZALES	JUDY1	29.521181	-97.245064
4217730798	GONZALES	ROBERT_BORRER1	29.763662	-97.354713
4217730885	GONZALES	IBARRA1	29.756018	-97.298233
4217730889	GONZALES	BVC	29.357943	-97.406998
4217730910	GONZALES	SPAHN1	29.556543	-97.487404
4217730905	GONZALES	ILEY_BW1	29.531271	-97.472923
4217730963	GONZALES	ROSANKY_JEWEL1	29.647409	-97.281784
4217731026	GONZALES	MOORE1	29.533867	-97.495262
4217731031	GONZALES	GANNON_UNIT1	29.697289	-97.239792
4217731070	GONZALES	KALKA_ALICE_M1	29.566429	-97.390541
4217731158	GONZALES	W_JEWEL_ETAL1	29.290771	-97.579781
4217731213	GONZALES	BOYSEN_MO1	29.494867	-97.501122
4217731258	GONZALES	BRYANT_SIDETRACK1	29.71771	-97.308327
4217731533	GONZALES	BROWN_BREWSTER1	29.414721	-97.699425

4217731547	GONZALES	BAKER1	29.316879	-97.369705
4217731604	GONZALES	COOK_JOHN_D_UNIT1	29.443434	-97.507187
4217731641	GONZALES	PLOEGER1	29.429989	-97.540573
4217731643	GONZALES	SPOHLER_ALFRED_B1	29.607504	-97.407104
4217731671	GONZALES	ELVIA1	29.561281	-97.481392
4218730886	GUADALUPE	KRAFT_#1	29.6476147	-98.117389
4218731672	GUADALUPE	#1_FOSTER	29.7409752	-97.840811
4218732024	GUADALUPE	KUSCHER_#1	29.7540728	-97.937153
4218732654	GUADALUPE	Sue_#47	29.5588008	-97.787806
4218733212	GUADALUPE	Thomas_B-24	29.606715	-97.746367
4218733229	GUADALUPE	ALLEN_A48	29.6979746	-97.756177
4218733264	GUADALUPE	#6	29.409752	-98.02596
4218732854	GUADALUPE	MD_#1	29.481035	-98.05008
4218732601	GUADALUPE	DOLLE _#1	29.568396	-97.869286
4218731063	GUADALUPE	PERRY1	29.504824	-97.783424
4218732394	GUADALUPE	1_WEINERT	29.409468	-97.89267
4218733009	GUADALUPE	SCHROEDER1	29.525387	-97.903244
4218733244	GUADALUPE	BALL_UNIT1	29.489632	-97.946053
4218733257	GUADALUPE	L_MARINES_NO29	29.684006	-97.763802
4218733293	GUADALUPE	MARTIN_BOOTH_UNIT	29.401442	-97.846123
4218733310	GUADALUPE	DINGLER_BATEY_#1	29.41596	-97.820839
4218733373	GUADALUPE	DAVENPORT_UNIT1	29.418877	-97.836105
4225530721	KARNES	JLM_1	28.924307	-98.027641

4225530854	KARNES	1_NANCE	29.190283	-97.709045
4225531043	KARNES	RIEDEL_1	29.120239	-97.772903
4225531209	KARNES	P1	28.938982	-97.994362
4225531488	KARNES	CHU_1	28.903749	-98.050972
4225531082	KARNES	RN1	28.744844	-97.910004
4225531091	KARNES	RGU_1	28.73654	-97.935463
4225530657	KARNES	IPC1	28.831215	-97.827744
4225531170	KARNES	HJ1	28.770966	-97.892334
4225531195	KARNES	CIP2	28.833771	-97.835892
4225531196	KARNES	BERRY_1	28.763498	-97.895538
4225531198	KARNES	CIP3	28.829018	-97.834053
4225531284	KARNES	HS1	28.883551	-97.784798
4225531368	KARNES	B1H	28.908009	-97.671791
4225531370	KARNES	D1H	28.909525	-97.679665
4225531471	KARNES	SFP	28.908749	-97.766258
4225531494	KARNES	RT3H	28.852625	-97.726524
4228732583	LEE	GAC_III	30.467499	-97.03283
4228732547	LEE	K1H	30.31348	-96.92669
4228730986	LEE	CHF_#1	30.362936	-96.98792
4228731959	LEE	GBU_#1	30.18093	-96.96433
4228731020	LEE	FWG_#1	30.153072	-96.80481
4228731178	LEE	SB_#1	30.209747	-96.90204
4249330995	WILSON	OLD_KING_1	29.17087	-97.937965

4249332588	WILSON	KELLER_#1H	29.111048	-97.99536
4249331544	WILSON	#1_Schneider	28.982702	-98.261795
4249332095	WILSON	POSEY_#1	29.244211	-97.97305
4249332189	WILSON	THOMS_#3B	29.019655	-98.160545
4249331840	WILSON	KOLLMAN_#1	29.129362	-97.85478
4249330680	WILSON	COPELAND_WE_ETL	29.077709	-98.120857
4249330736	WILSON	MOCZYGEMBA	29.033371	-98.018112
4249330748	WILSON	BRYAN_ES	28.967232	-98.261177
4249330769	WILSON	BUDEWIG_ESTATE	29.036121	-98.068115
4249330785	WILSON	PAWELEK	28.985048	-98.205017
4249330798	WILSON	COMPTON_OD	29.161922	-98.063683
4249331024	WILSON	MENGDEN_P_ETAL	28.992704	-98.155968
4249331061	WILSON	1_SWIENTEK	29.114004	-98.072456
4249331239	WILSON	FWNB1	29.046434	-98.329391
4249331282	WILSON	SM_LANGILL_ESTATE	29.134634	-98.062943
4249331431	WILSON	HEWELL_WW_ETAL	29.308992	-97.853226
4249331544	WILSON	SCHNEIDER	28.982702	-98.261795
4249331898	WILSON	1_STADLER	29.151381	-98.019691
4249331673	WILSON	JOST_ALFRED_C1	29.306557	-97.854729
4249331745	WILSON	PERKINS_E1	29.099211	-98.111816
4249331786	WILSON	HEWELL_WW3	29.312326	-97.851463
4249331829	WILSON	PROSPER_LABUS	28.991322	-98.150917
4249332046	WILSON	FINCH_BIRD	29.287535	-97.913391

4249332100	WILSON	LEHMANN_UNIT1	29.120464	-98.195923
4249332179	WILSON	SETLIFF1	29.280499	-97.84388
4249332182	WILSON	BRYAN1	29.056683	-98.242256
4249332190	WILSON	THOMS2	29.005268	-98.122124
4249332395	WILSON	ALMA_LOPEZ	29.156715	-98.018013
4249332489	WILSON	MCCLOSKEY__ETAL1	29.187737	-98.083778

APPENDIX B

CORE FEATURES

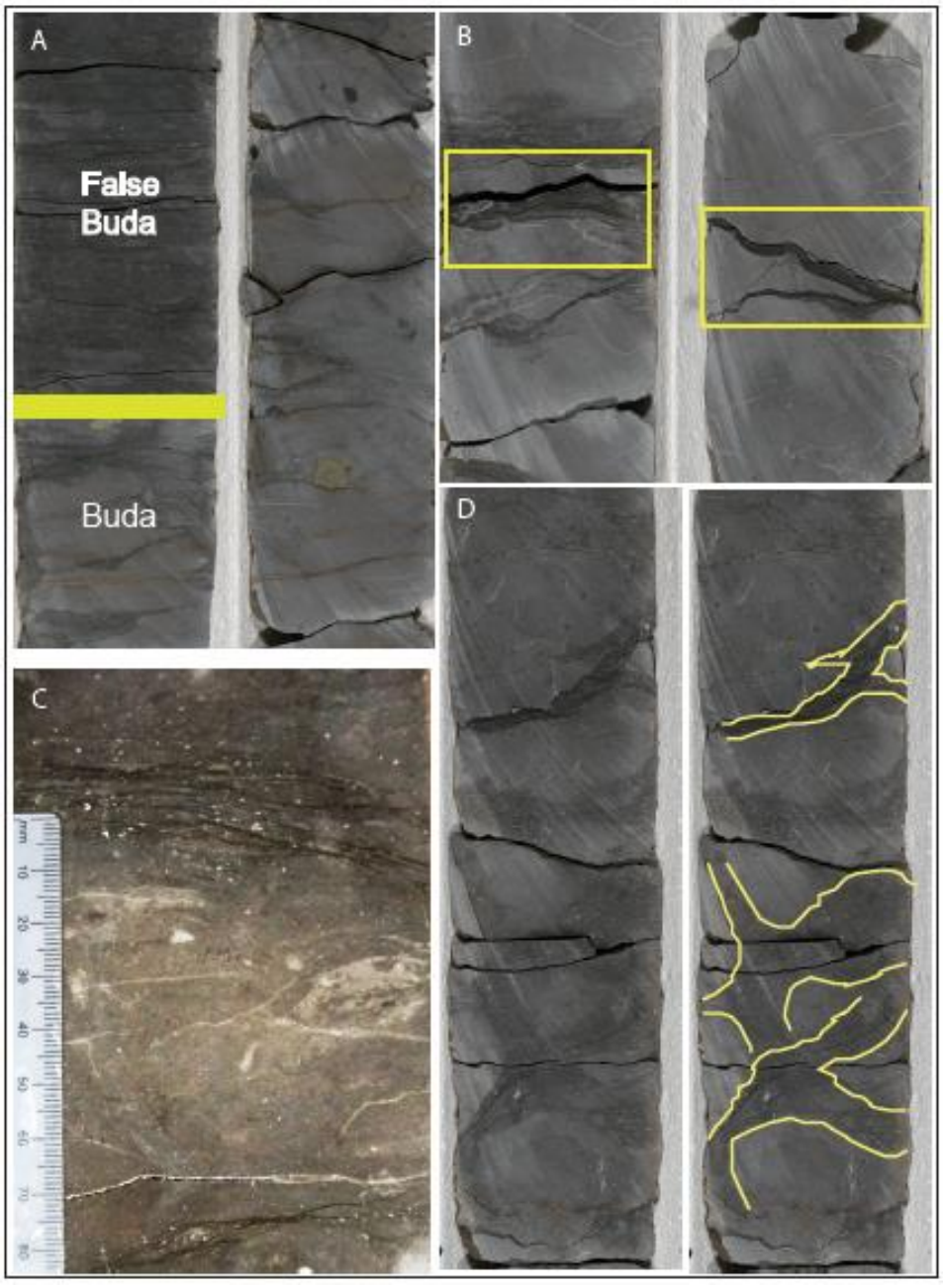

A1**.** Buda Formation and False Buda unit core features. A. Gradual contact of False Buda and Buda in the core. B. Thin shale seams observed in the core of Buda Formation. C. Bioturbated bedding of the Buda Formation. D. Nodular bedding within the Buda Formation